Global fit of Non-relativistic Effective Operator Dark Matter using Solar Neutrinos

Neal Avis Kozar

Aaron Vincent

Work with Aaron Vincent, Pat Scott, and help from the GAMBIT collaboration

AUGUST 11, 2022

TeVPA

Queen's University

Talk Summary

Introduction

Dark Matter Candidates

- Dark matter is known to interact gravitationally
- Otherwise the parameter space is open to search
- This work focuses on the WIMP

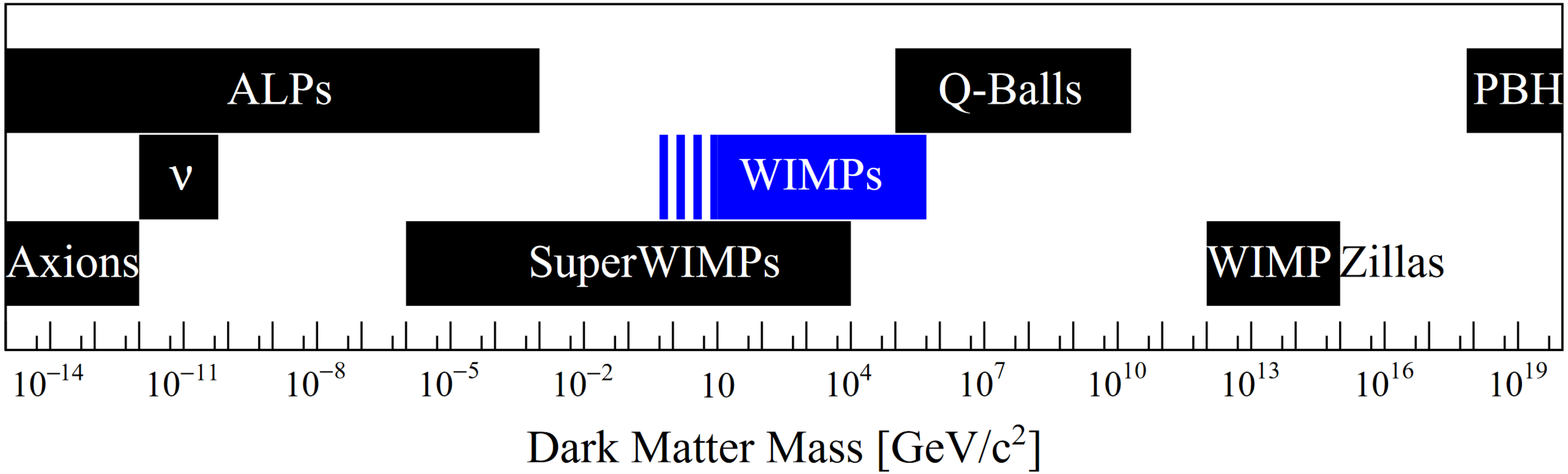

[1]

Queen's University

Search Types

- Indirect detection, direct detection, collider searches
- Each are independent detection methods
- Solar neutrinos act as a compliment to direct detection

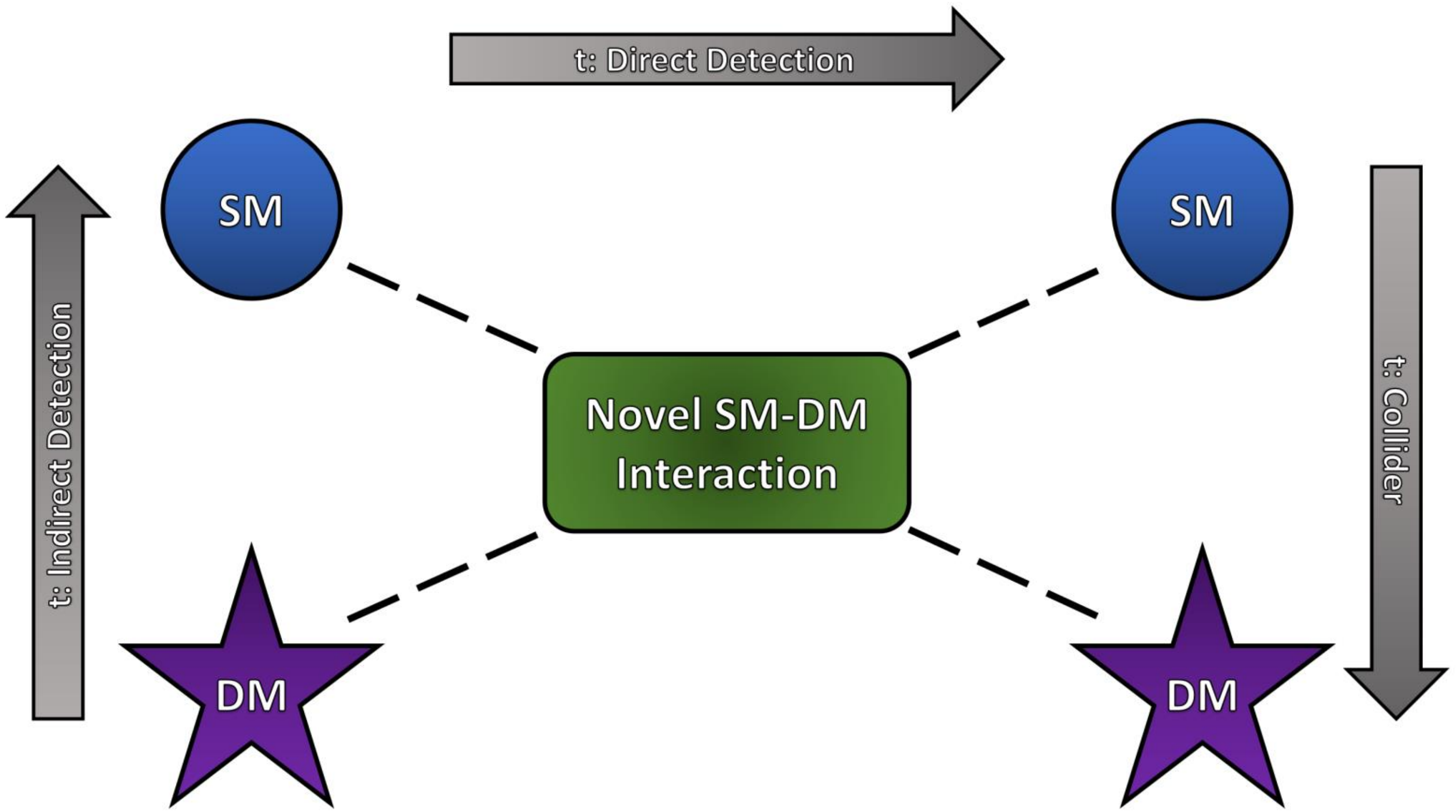

Direct Detection

- The goal is to detect the recoil of nuclei from dark matter interactions
- Parametrized into two cases:
  - Spin-dependent, coupling to the overall spin of nuclei
  - Spin-independent, which receives a coupling enhancement for higher mass nuclei

$$\sigma_{SI} = \frac{\mu^2}{\mu_n^2} A^2 \sigma_n$$

Advantages of an Effective Field Theory

- High-energy theory parametrization
- Fitzpatrick et. al. [2] describe a toy model dark matter effective field theory
- Dark matter substructure can be ignored at galactic halo velocities

$$\hat{\mathbf{q}}_{\max} = 200 \text{ MeV}$$

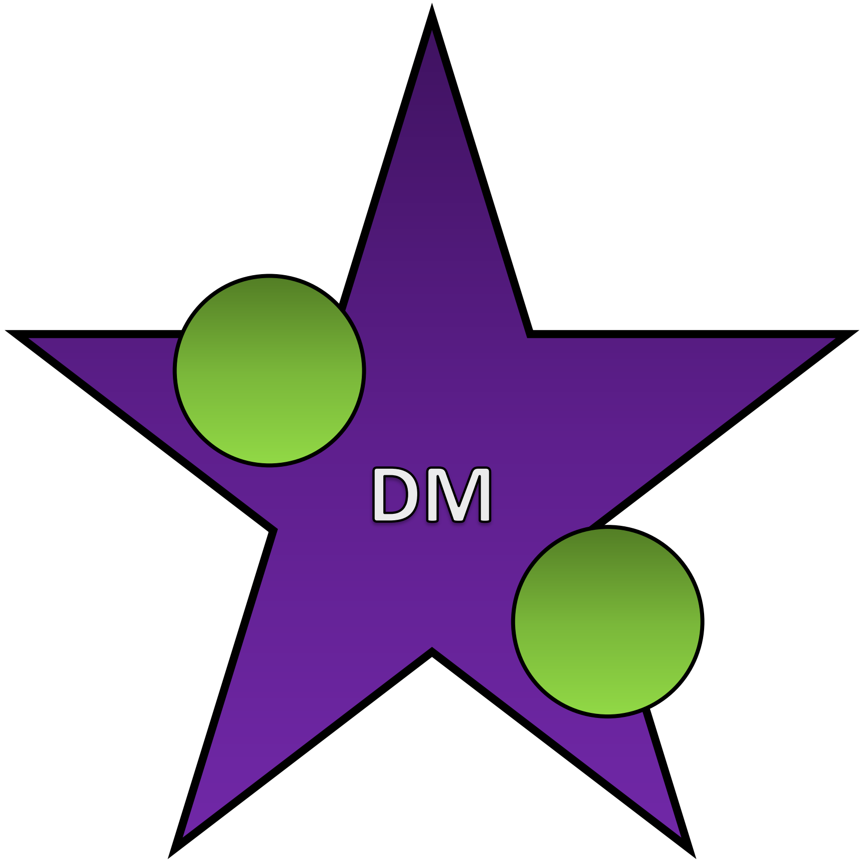

Hermitian Operators

- The general case of a dark matter scattering interaction is considered
- The Hermitian operators that govern the interaction are

$$\mathbb{1}_{\chi N} \quad , \quad i\hat{\mathbf{q}} \quad , \quad \hat{\mathbf{v}}^{\perp} \quad , \quad \hat{\mathbf{S}}_{\chi} \quad , \quad \hat{\mathbf{S}}_{N}$$

$$\hat{\mathbf{v}}^{\perp} = \hat{\mathbf{v}} + \hat{\mathbf{q}}/(2\mu_N)$$

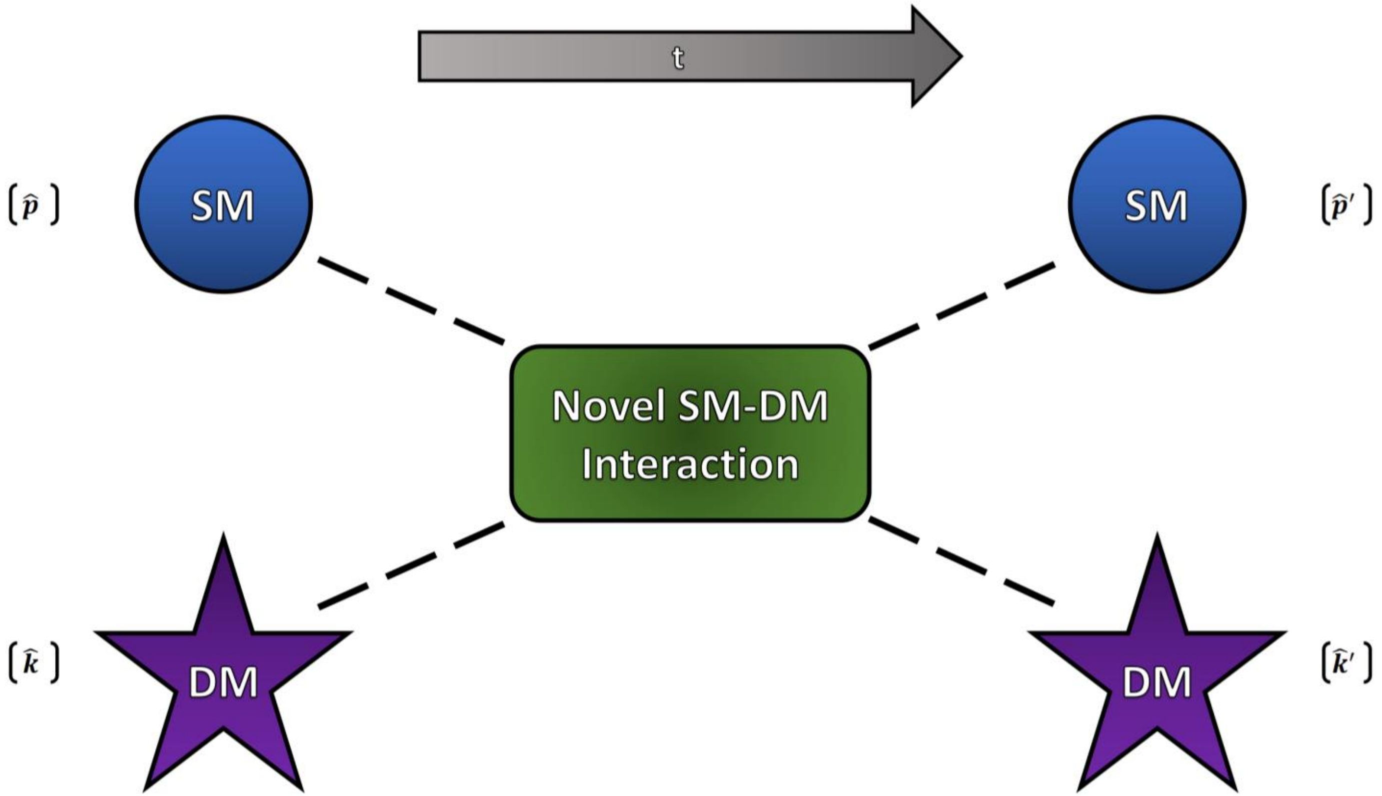

Non-Relativistic Effective Operators

- Spin-independent: $\hat{\mathcal{O}}_1 = \mathbb{1}_{\chi N}$
- Spin-dependent: $\hat{\mathcal{O}}_4 = \hat{\mathbf{S}}_\chi \cdot \hat{\mathbf{S}}_N$
- Novel interactions, such as

$$\hat{\mathcal{O}}_{10} = i\hat{\mathbf{S}}_N \cdot \frac{\hat{\mathbf{q}}}{m_N}$$

- Acts as leading contributor to higher-energy theories [3]:

$$\mathcal{L} \supset \lambda_1 \phi \bar{\chi} \chi - i h_2 \phi \bar{q} \gamma^5 q \to \hat{\mathcal{H}} \supset \left(c_{10}^0 t^0 + c_{10}^1 t^1\right) \hat{\mathcal{O}}_{10}$$

$\hat{\mathcal{O}}_1 = \mathbb{1}_{\chi N}$	$\hat{\mathcal{O}}_9 = i\hat{\mathbf{S}}_\chi \cdot \left(\hat{\mathbf{S}}_N \times \frac{\hat{\mathbf{q}}}{m_N}\right)$
$\hat{\mathcal{O}}_2 = \hat{\mathbf{v}}^\perp \cdot \hat{\mathbf{v}}^\perp$	$\hat{\mathcal{O}}_{10} = i\hat{\mathbf{S}}_N \cdot \frac{\hat{\mathbf{q}}}{m_N}$
$\hat{\mathcal{O}}_3 = i\hat{\mathbf{S}}_N \cdot \left(\frac{\hat{\mathbf{q}}}{m_N} \times \hat{\mathbf{v}}^\perp\right)$	$\hat{\mathcal{O}}_{11} = i\hat{\mathbf{S}}_\chi \cdot \frac{\hat{\mathbf{q}}}{m_N}$
$\hat{\mathcal{O}}_4 = \hat{\mathbf{S}}_\chi \cdot \hat{\mathbf{S}}_N$	$\hat{\mathcal{O}}_{12} = \hat{\mathbf{S}}_\chi \cdot \left(\hat{\mathbf{S}}_N \times \hat{\mathbf{v}}^\perp\right)$
$\hat{\mathcal{O}}_5 = i\hat{\mathbf{S}}_\chi \cdot \left(\frac{\hat{\mathbf{q}}}{m_N} \times \hat{\mathbf{v}}^\perp\right)$	$\hat{\mathcal{O}}_{13} = i\left(\hat{\mathbf{S}}_\chi \cdot \hat{\mathbf{v}}^\perp\right)\left(\hat{\mathbf{S}}_N \cdot \frac{\hat{\mathbf{q}}}{m_N}\right)$
$\hat{\mathcal{O}}_6 = \left(\hat{\mathbf{S}}_\chi \cdot \frac{\hat{\mathbf{q}}}{m_N}\right)\left(\hat{\mathbf{S}}_N \cdot \frac{\hat{\mathbf{q}}}{m_N}\right)$	$\hat{\mathcal{O}}_{14} = i\left(\hat{\mathbf{S}}_\chi \cdot \frac{\hat{\mathbf{q}}}{m_N}\right)\left(\hat{\mathbf{S}}_N \cdot \hat{\mathbf{v}}^\perp\right)$
$\hat{\mathcal{O}}_7 = \hat{\mathbf{S}}_N \cdot \hat{\mathbf{v}}^\perp$	$\hat{\mathcal{O}}_{15} = -\left(\hat{\mathbf{S}}_\chi \cdot \frac{\hat{\mathbf{q}}}{m_N}\right)\left[\left(\hat{\mathbf{S}}_N \times \hat{\mathbf{v}}^\perp\right) \cdot \frac{\hat{\mathbf{q}}}{m_N}\right]$
$\hat{\mathcal{O}}_8 = \hat{\mathbf{S}}_\chi \cdot \hat{\mathbf{v}}^\perp$	

Cross Section

- Cross section becomes a large sum over response functions

$$\frac{\mathrm{d}\sigma_i}{\mathrm{d}E}(w^2, q^2) = \frac{m_T}{2\pi w^2} P_{\mathrm{tot}}(w^2, q^2)$$

$$\begin{aligned} P_{\mathrm{tot}}(w^2, q^2) = \frac{4\pi}{2J+1} \sum_{\tau=0,1} \sum_{\tau'=0,1} \Bigg\{ \Bigg[& R_M^{\tau\tau'}\left(v_T^{\perp 2}, \frac{q^2}{m_N^2}\right) W_M^{\tau\tau'}(y) \\ & + R_{\Sigma''}^{\tau\tau'}\left(v_T^{\perp 2}, \frac{q^2}{m_N^2}\right) W_{\Sigma''}^{\tau\tau'}(y) + R_{\Sigma'}^{\tau\tau'}\left(v_T^{\perp 2}, \frac{q^2}{m_N^2}\right) W_{\Sigma'}^{\tau\tau'}(y) \Bigg] \\ & + \frac{q^2}{m_N^2} \Bigg[R_{\Phi''}^{\tau\tau'}\left(v_T^{\perp 2}, \frac{q^2}{m_N^2}\right) W_{\Phi''}^{\tau\tau'}(y) + R_{\Phi'' M}^{\tau\tau'}\left(v_T^{\perp 2}, \frac{q^2}{m_N^2}\right) W_{\Phi'' M}^{\tau\tau'}(y) \\ & + R_{\tilde{\Phi}'}^{\tau\tau'}\left(v_T^{\perp 2}, \frac{q^2}{m_N^2}\right) W_{\tilde{\Phi}'}^{\tau\tau'}(y) + R_{\Delta}^{\tau\tau'}\left(v_T^{\perp 2}, \frac{q^2}{m_N^2}\right) W_{\Delta}^{\tau\tau'}(y) \\ & + R_{\Delta\Sigma'}^{\tau\tau'}\left(v_T^{\perp 2}, \frac{q^2}{m_N^2}\right) W_{\Delta\Sigma'}^{\tau\tau'}(y) \Bigg] \Bigg\} \end{aligned}$$

- Effective Cross section

$$\sigma_p = \frac{\left(c_i^\tau \mu_n\right)^2}{\pi}$$

Solar Capture

Capture Process

- Dark matter is captured when it scatters to below the local escape velocity in the Sun

$$C = 4\pi \int_0^{R_\odot} \mathrm{d}R R^2 \int_0^\infty \mathrm{d}u \frac{f(u)}{u} w \Omega_v^-(w)$$

$$\Omega_v^-(w) = \sum_i n_i w \Theta\left(\frac{\mu_i}{\mu_{+,i}^2} - \frac{u^2}{w^2}\right) \int_{E_k u^2/w^2}^{E_k \mu_i/\mu_{+,i}^2} \mathrm{d}E_R \frac{\mathrm{d}\sigma_i}{\mathrm{d}E_R}\left(w^2, q^2\right)$$

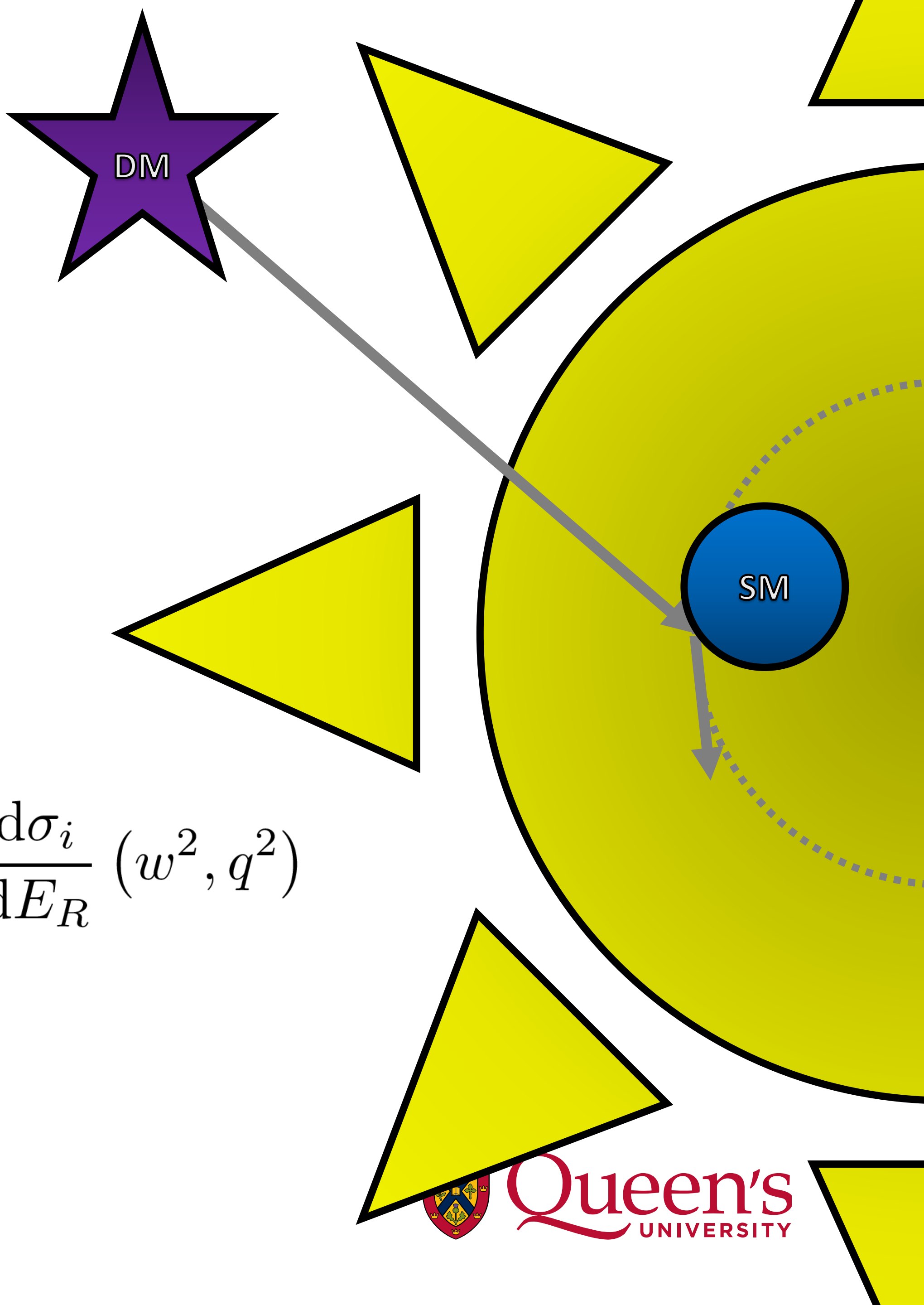

Geometric Limit

- The Sun has a hard limit of dark matter capture

$$C_{\max}(t) = \pi R_{\odot}^2(t) \int_0^{\infty} \frac{f_{\odot}(u)}{u} w^2(u, R_{\odot}) \mathrm{d}u$$

$$C_{\max}(t) = \frac{1}{3}\pi \frac{\rho_\chi}{m_\chi} R_{\odot}^2(t) \left(e^{-\frac{3}{2}\frac{u_{\odot}^2}{u_0^2}} \sqrt{\frac{6}{\pi}} u_0 + \frac{6G_{\mathrm{N}} M_{\odot} + R_{\odot}(u_0^2 + 3u_{\odot}^2)}{R_{\odot} u_{\odot}} \mathrm{Erf}\left[\sqrt{\frac{3}{2}} \frac{u_{\odot}}{u_0} \right] \right)$$

- We take minimum of the limit and capture rate

Annihilation in the Sun

- The number density of dark matter is given by

$$\frac{\mathrm{d}N_\chi(t)}{\mathrm{d}t} = C(t) - A(t) - E(t) = 0$$

- At steady state, the annihilation rate only depends on the capture:

$$\Gamma_A = (C/2)\tanh^2(t/\tau)$$

- The final neutrino flux is found from branching ratios

$$\frac{\mathrm{d}\Phi_\nu}{\mathrm{d}E_\nu} = \frac{\Gamma_A}{4\pi D^2}\sum_f B_\chi^f \frac{\mathrm{d}N_\nu^f}{\mathrm{d}E_\nu}$$

Queen's UNIVERSITY

Other Applications

- The same calculation in other stars can be performed
  - There is current work to integrate with DarkMESA

- Can look at other phenomena like
  - Energy transport [4,5]
  - Modified main sequence lifetimes [6]
  - Triggering thermonuclear explosions in stellar remnants [7-9]

Capt'n General

- Capt'n [10] was designed for capture rate calculations
  - As standalone
  - GAMBIT backend
  - DarkMESA companion

- Capt'n uses several parameters to calculate the DM capture rate in s^{-1}
  - Solar model including isotopic abundances
  - Dark matter halo parameters
  - Interaction model

GAMBIT

GAMBIT

- GAMBIT [11] combines many separate branches of physics to perform global scans of novel physics using existing experimental data
- Modular design to promote contributions
- Global scans can pick out signals of new physics before single experiments

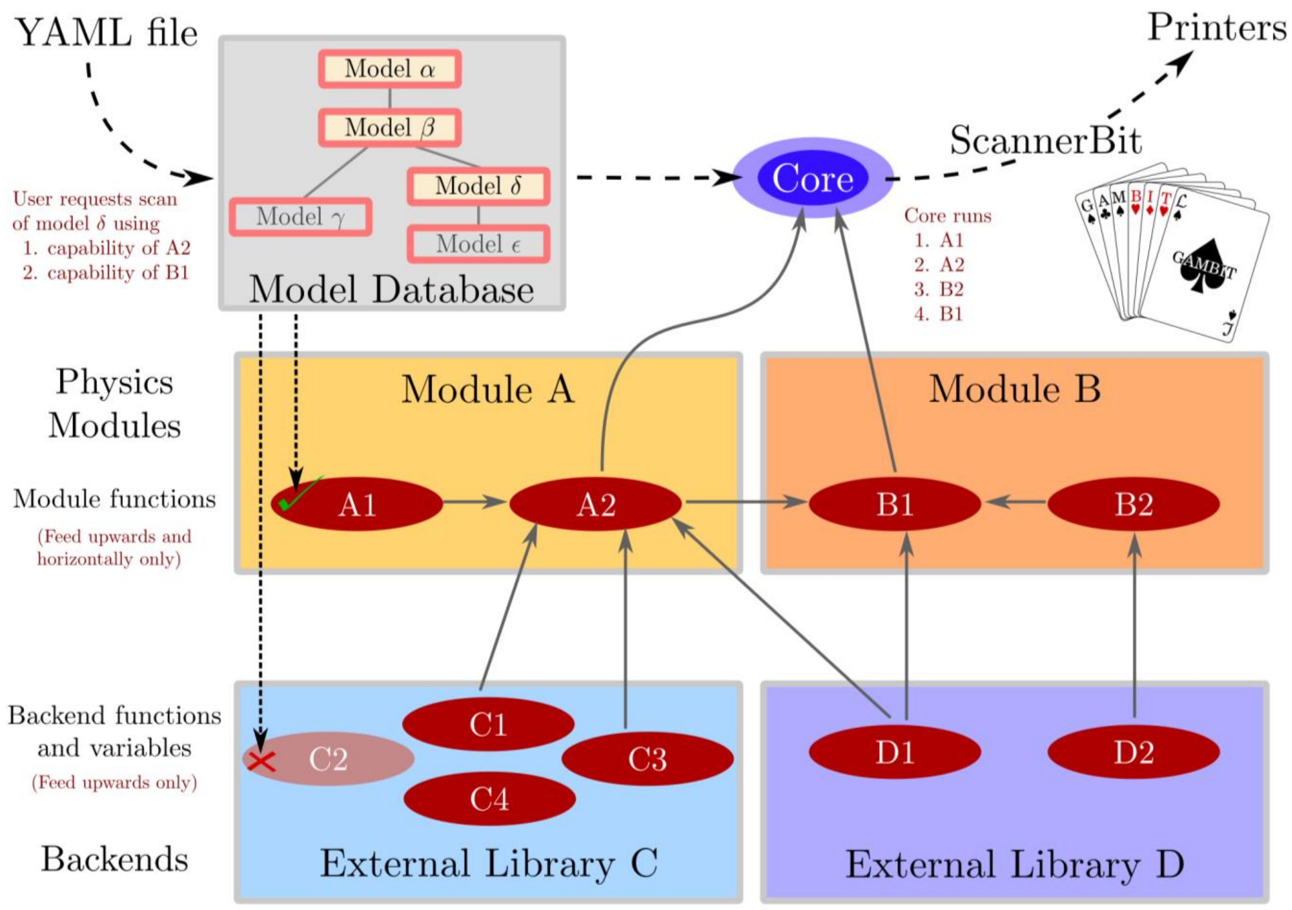

IceCube Neutrino Observatory

- For the 79-string run, IceCube's [12] digital optical modules were arranged as:
  - 73 strings with 125 m horizontal spacing and 17 m vertical spacing
  - 6 strings with less than 75 m horizontal spacing and 7 m vertical spacing in the DeepCore [13]
- The data is broken into three independent streams, of two varieties:
  - Low energy: exterior strings act as muon veto for the central array (Summer Low and Winter Low)
  - Higher energy: no restrictions (Winter High)
- IceCube performs better at higher-energy neutrino detection

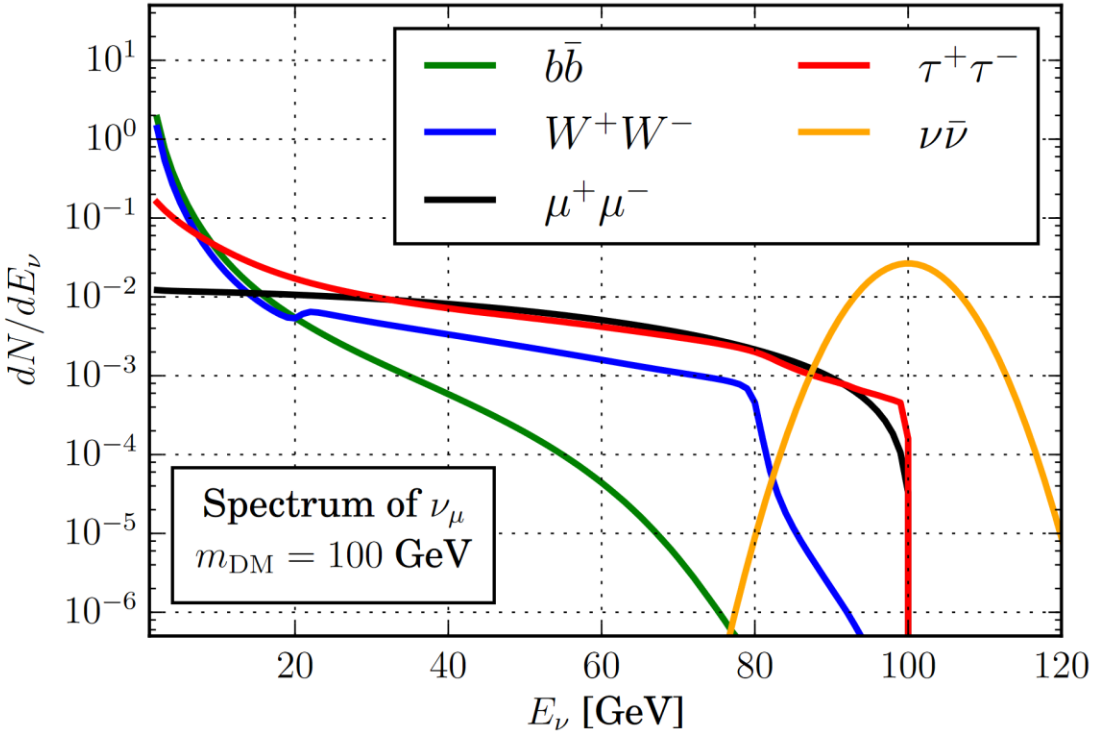

[14]

Direct Detection Experiments

- Eight direct detection experiments were included:
  - LUX 2016 [15]
  - XENON1T 2018 [16]
  - PandaX-II 2016 [17] and 2017 [18]
  - PICO-60 2017 [19]
  - CRESST-II [20]
  - CDMSlite [21]
  - DarkSide-50 [22]

- These are:
  - Dual-phase time projection chambers (LUX, XENON1T, PandaX-II, and DarkSide-50)
  - Super-heated fluorine (PICO-60)
  - Cryogenic crystal detectors (CRESST-II and CDMSlite)

Added Experiments

- Two extra experiments were included in a post processing run
  - ANTARES from Dark Ghosts 2022 presented by Chiara Poirè [23]
  - IceCube Update from Dark Ghosts 2022 presented by Stephan Meighen-Berger [24]

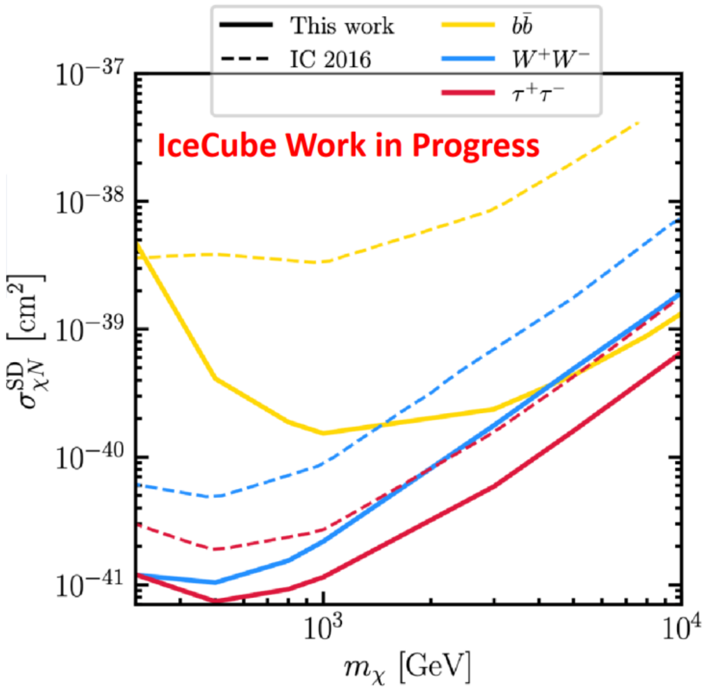

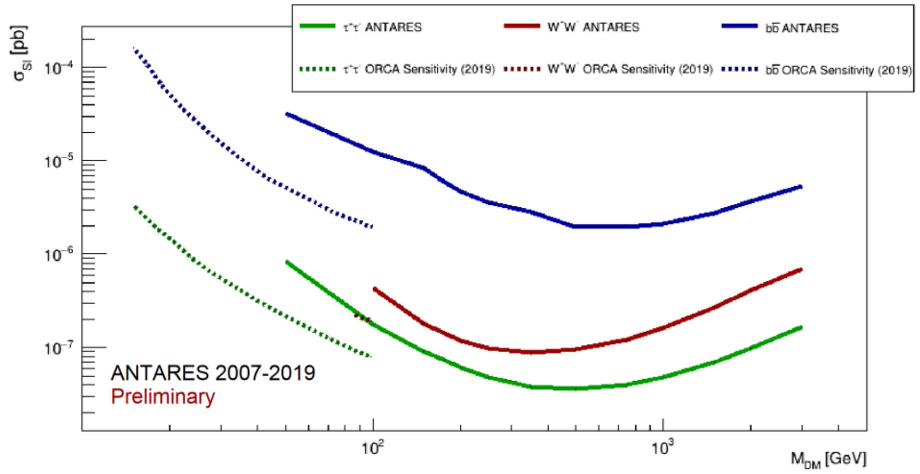

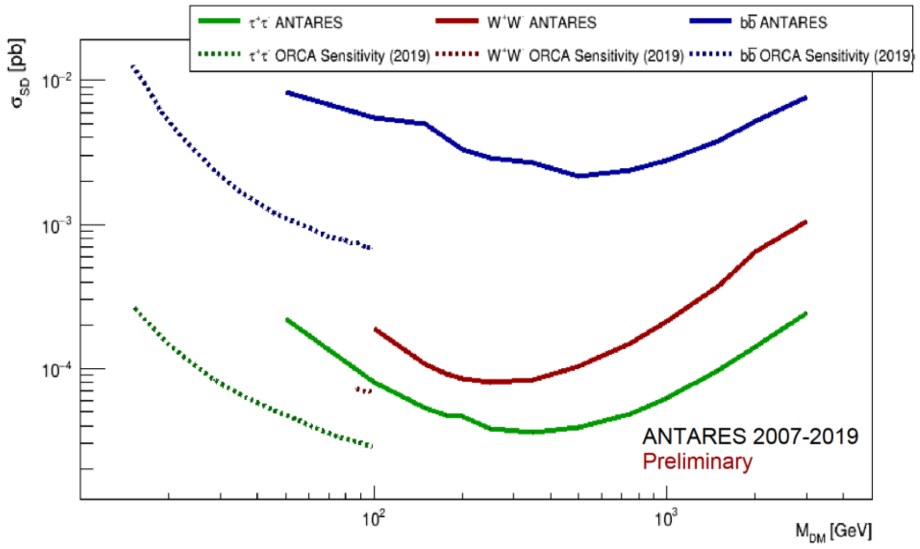

Queen's University

Scanning with Diver

- Diver is a differential evolution scanner in GAMBIT
- It can rapidly map likelihood contours
- But cannot give posteriors
- Differential evolution occurs in three steps
  - Mutation
  - Crossover
  - Selection

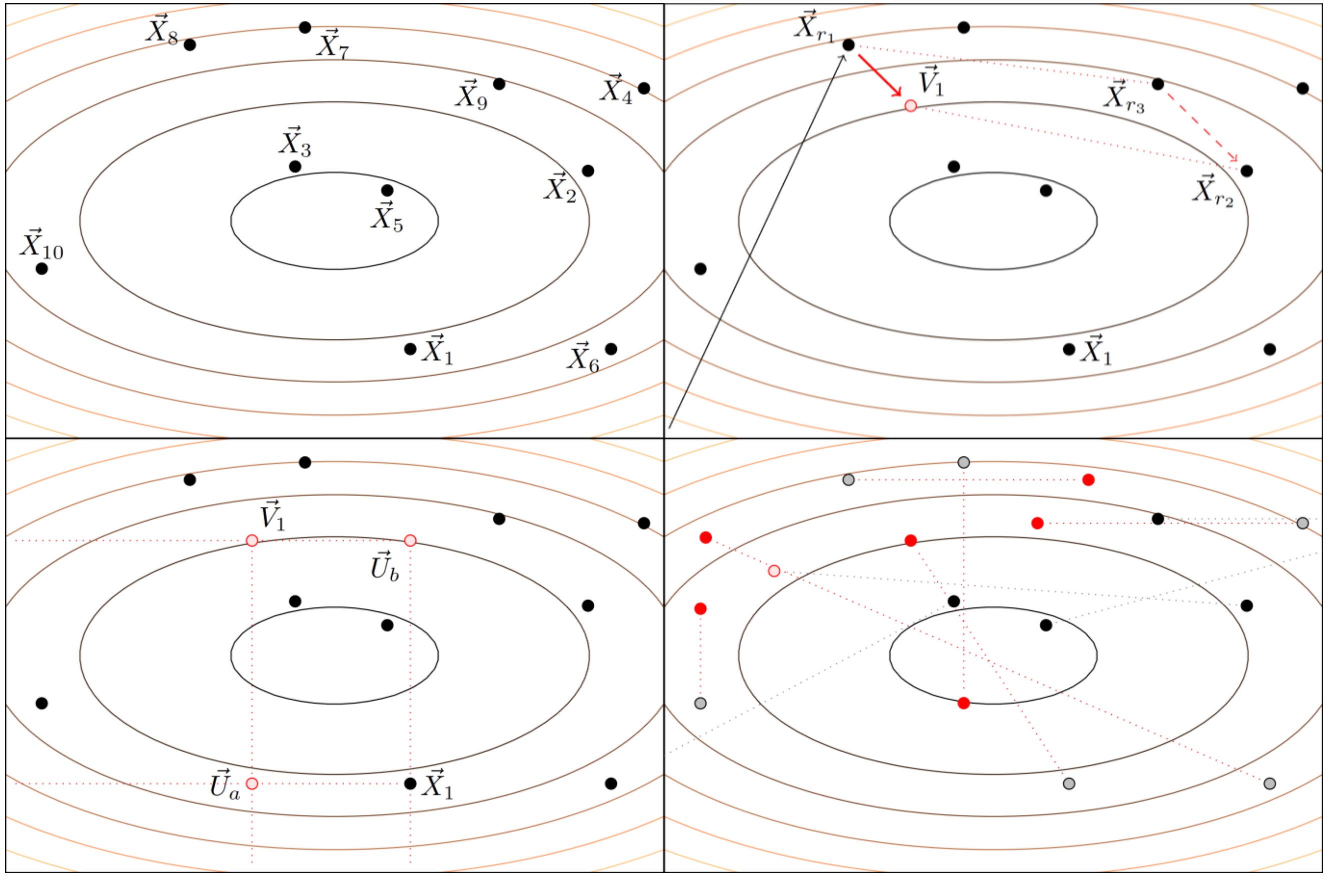

[25]

Results and Scans

Capt’n Capture Rates c_1 and c_4

- Capt’n can return capture rates per isotopic contribution
- Capt’n shows accuracy around ~5% of the previous Catena and Schwabe [26]

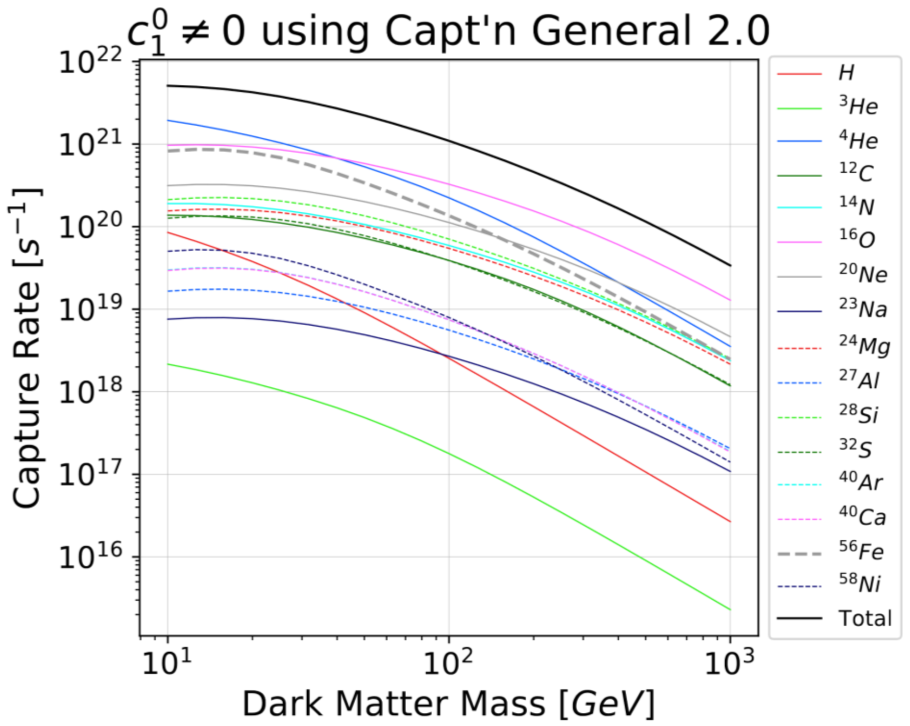

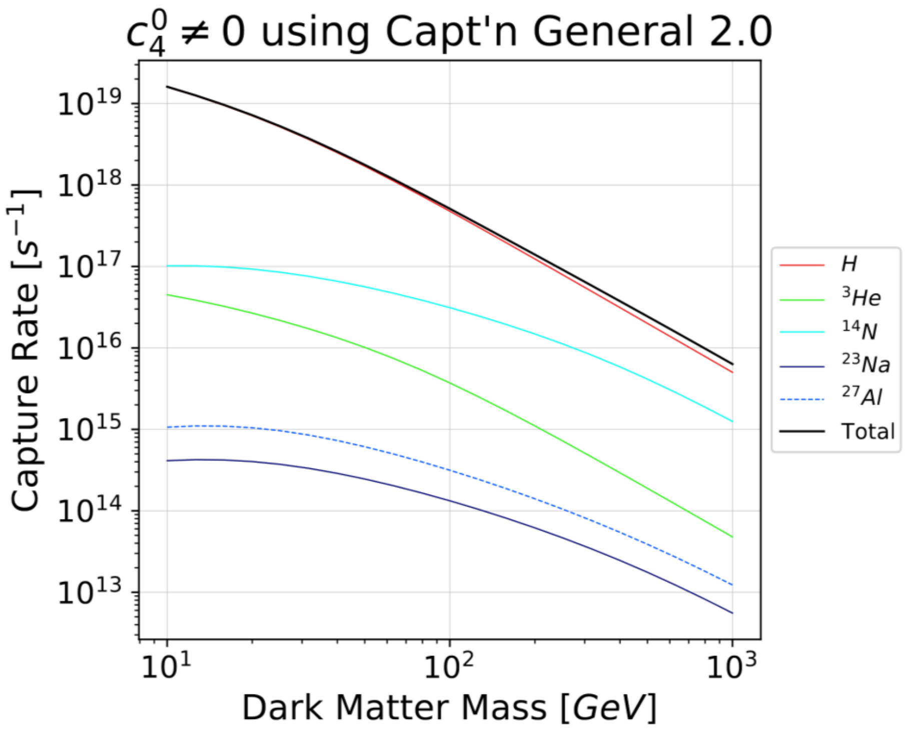

Queen's UNIVERSITY

Capt'n Capture Rates c_{10} and c_{11}

- Certain isotopes dominate depending on coupling

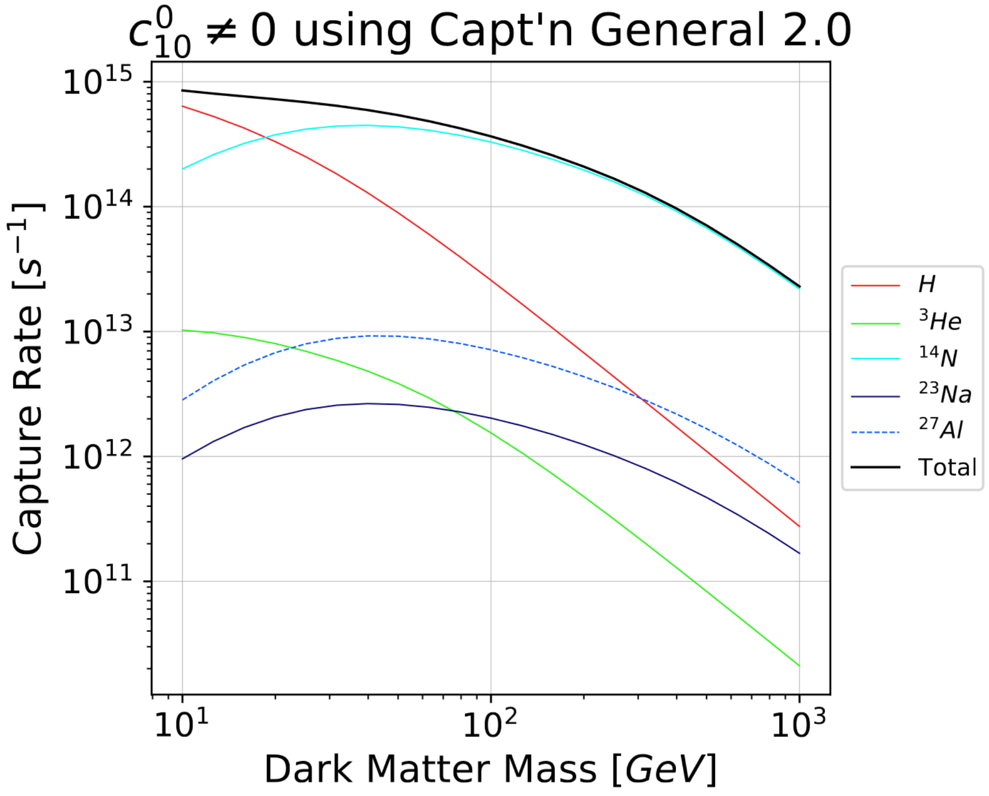

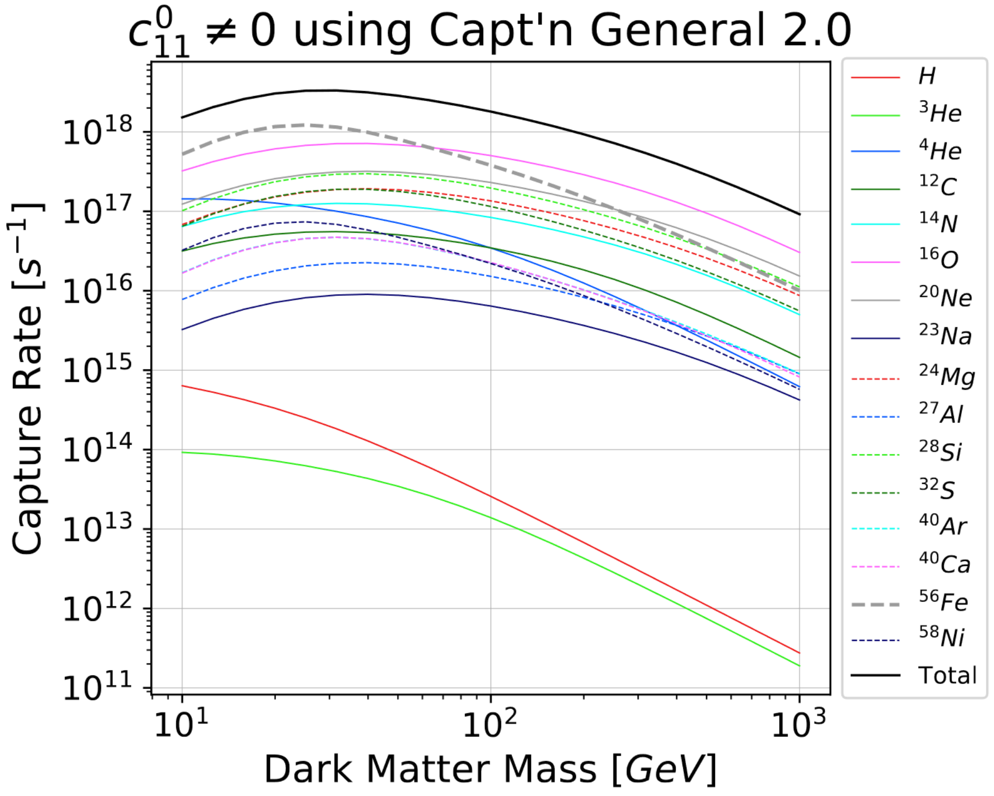

GAMBIT Scan Parameters

- The halo parameters are shared between all GAMBIT scans

Halo Parameters		Dark Matter Parameters	
ρ_0	0.5 GeV cm^{-3}	m_{dm}	$1 - 10^4$ GeV
v_0	$216 - 264$ km s^{-1}	c_1^0	$10^{-10} - 10^{-6}$ GeV^{-2}
v_{rot}	$216 - 264$ km s^{-1}	c_4^0	$10^{-8} - 10^{-4}$ GeV^{-2}
v_{esc}	$453 - 603$ km s^{-1}	c_{10}^0	$10^{-6} - 10^{-2}$ GeV^{-2}

- These scans are presented as profiled likelihoods with 90% C.L.
- All scans have 2 decay channel versions: $b\bar{b}$ and W^+W^-

Queen's UNIVERSITY

Spin-Independent and Spin-Dependent $b\bar{b}$ Channel

- The bottom quark annihilation channel for c_1 (left) and c_4 (right)
- Dominated by leading direct detection experiments

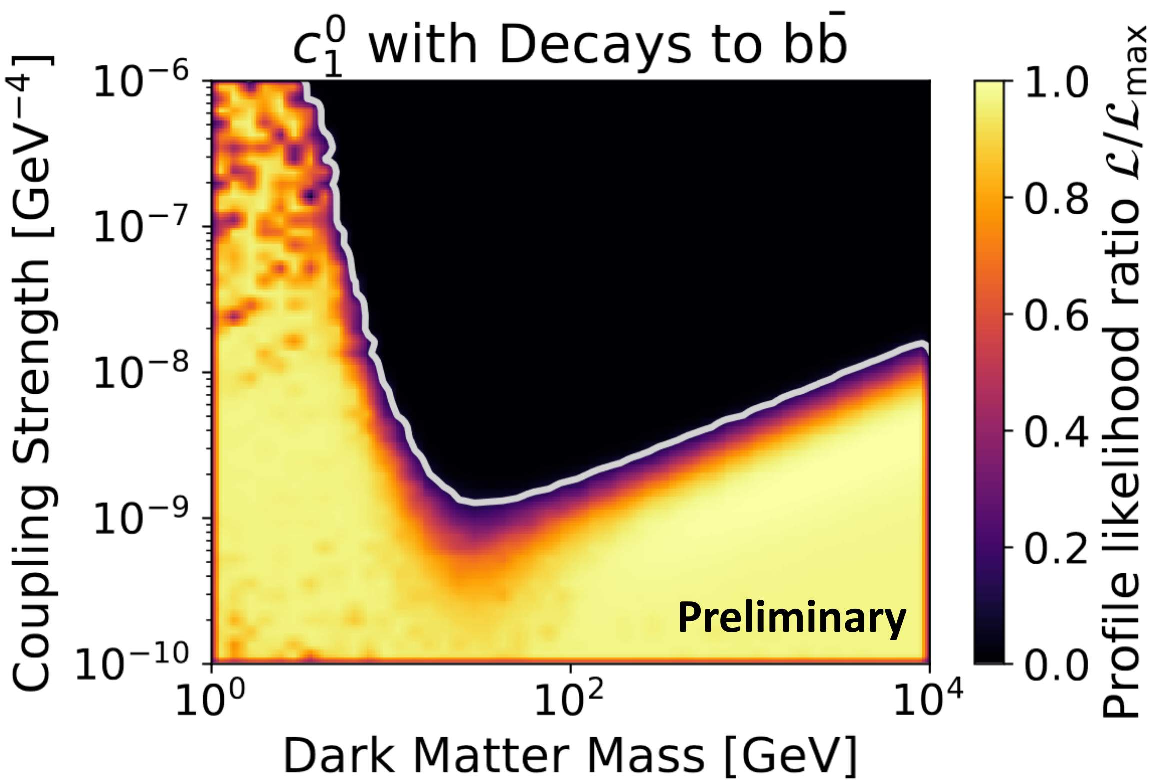

$$\hat{\mathcal{O}}_1 = \mathbb{1}_{\chi N}$$

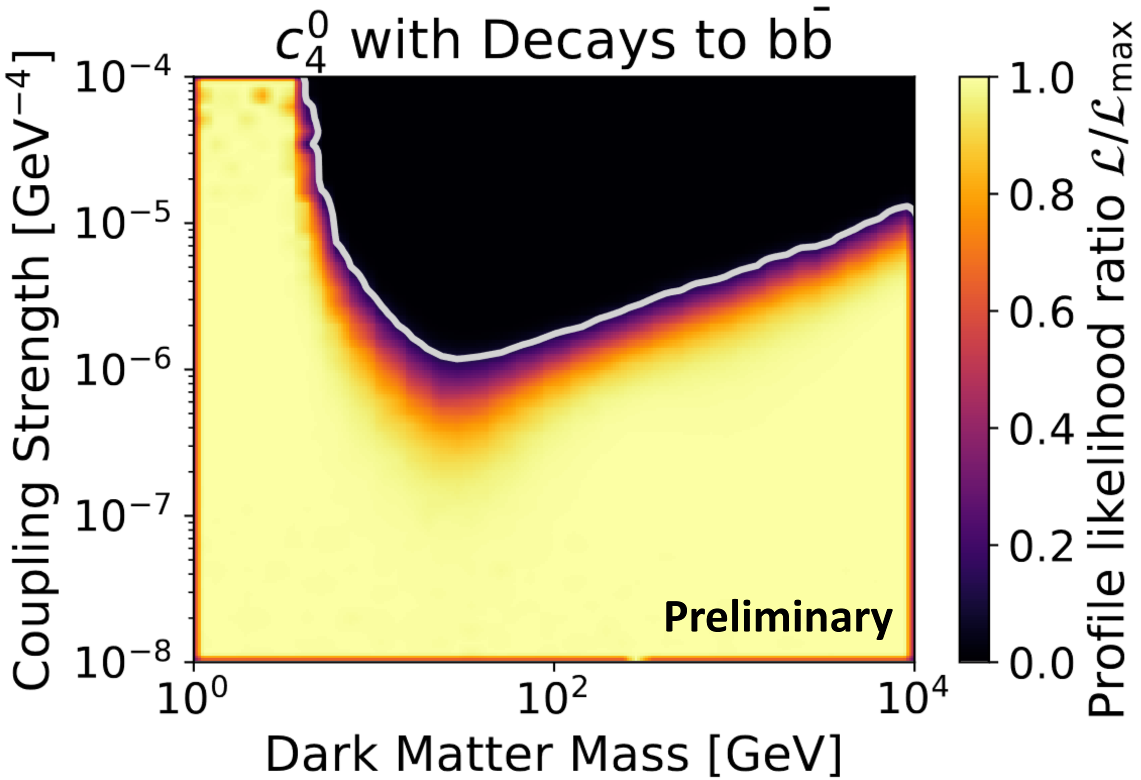

$$\hat{\mathcal{O}}_4 = \hat{\mathbf{S}}_\chi \cdot \hat{\mathbf{S}}_N$$

Queen's UNIVERSITY

Spin-Independent and Spin-Dependent $b\bar{b}$ Channel Breakdown

- The bottom quark annihilation channel for c_1 (left) and c_4 (right)
- Lead by XENON1T in spin-independent, and PICO-60 in spin-dependent

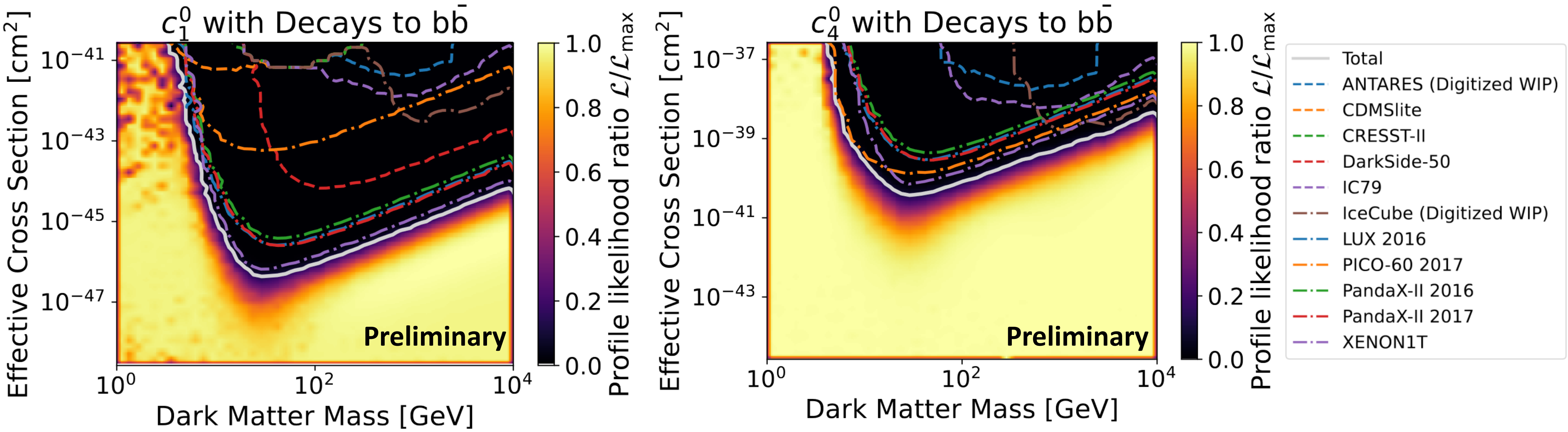

$\hat{\mathcal{O}}_1 = \mathbb{1}_{\chi N}$

$\hat{\mathcal{O}}_4 = \hat{\mathbf{S}}_\chi \cdot \hat{\mathbf{S}}_N$

Queen's UNIVERSITY

Spin-Independent and Spin-Dependent W^+W^- Channel

- The W boson annihilation channel for c_1 (left) and c_4 (right)
- Spin-dependent channel receives solar neutrino contribution

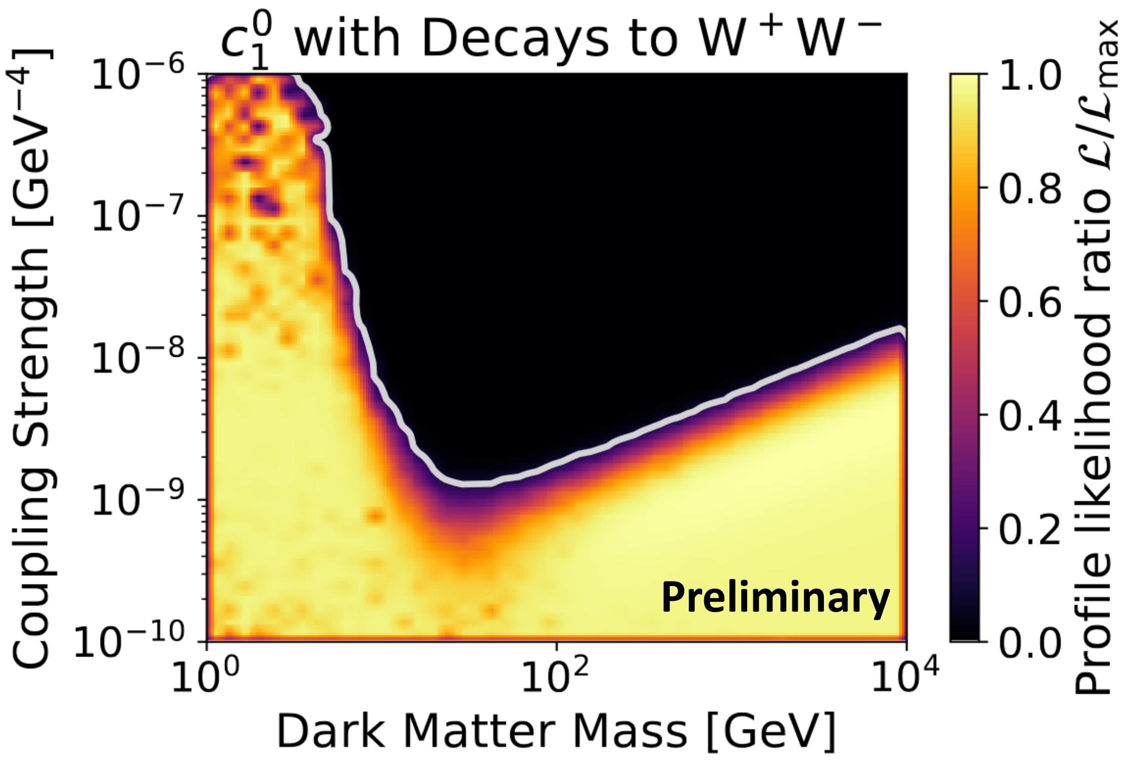

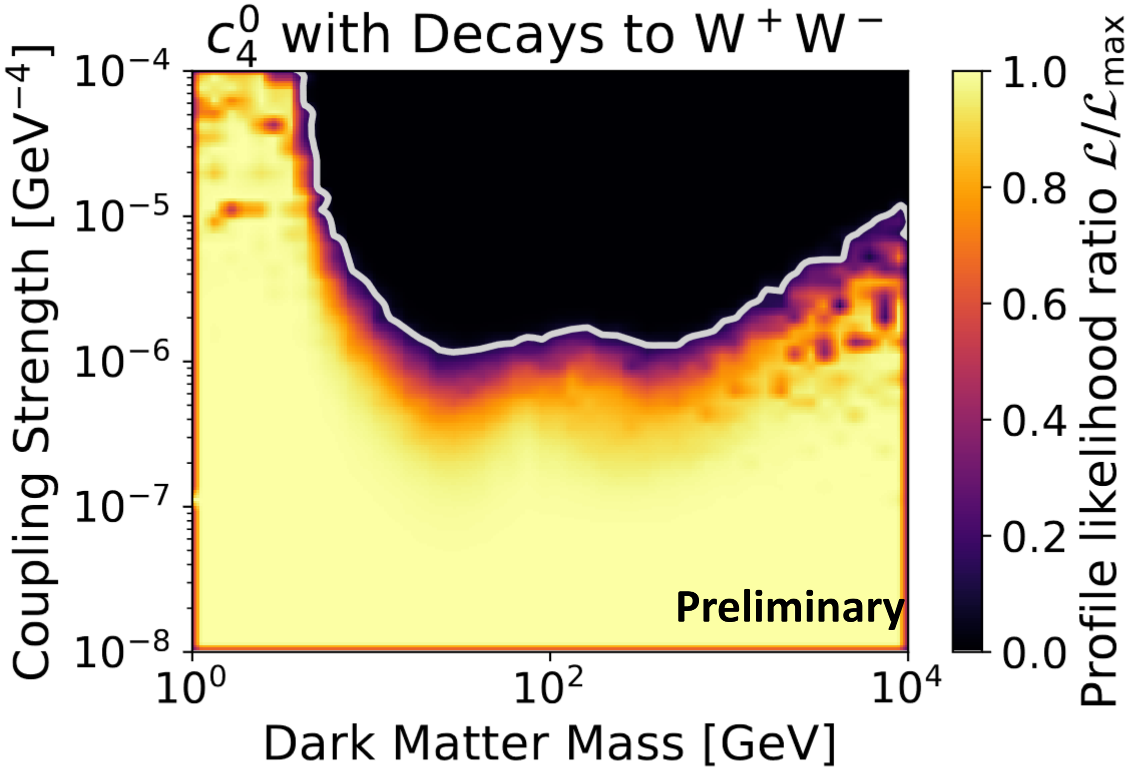

$$\hat{\mathcal{O}}_1 = \mathbb{1}_{\chi N}$$

$$\hat{\mathcal{O}}_4 = \hat{\mathbf{S}}_\chi \cdot \hat{\mathbf{S}}_N$$

Spin-Independent and Spin-Dependent W^+W^- Channel Breakdown

- The W boson annihilation channel for c_1 (left) and c_4 (right)
- IceCube out-competes in spin-dependent dark matter detection around ~500 GeV

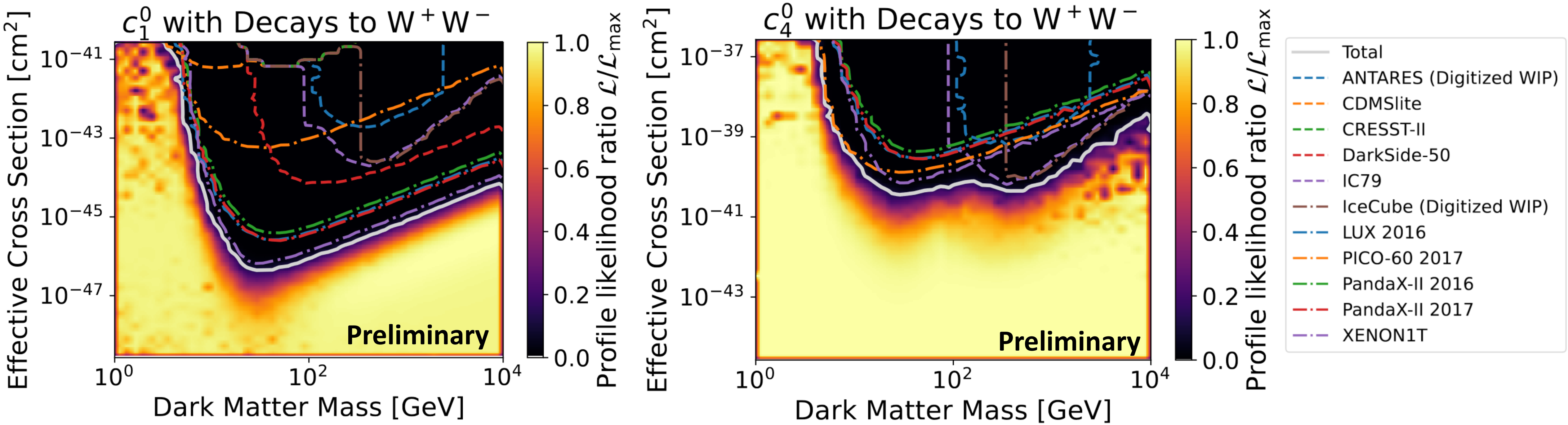

$$\hat{\mathcal{O}}_1 = \mathbb{1}_{\chi N}$$

$$\hat{\mathcal{O}}_4 = \hat{\mathbf{S}}_\chi \cdot \hat{\mathbf{S}}_N$$

Queen's UNIVERSITY

C_{10} Coupling Experiment Breakdown

- The W boson (right) and bottom quark annihilation channels for c_{10}
- W boson channel sees contribution from solar neutrinos

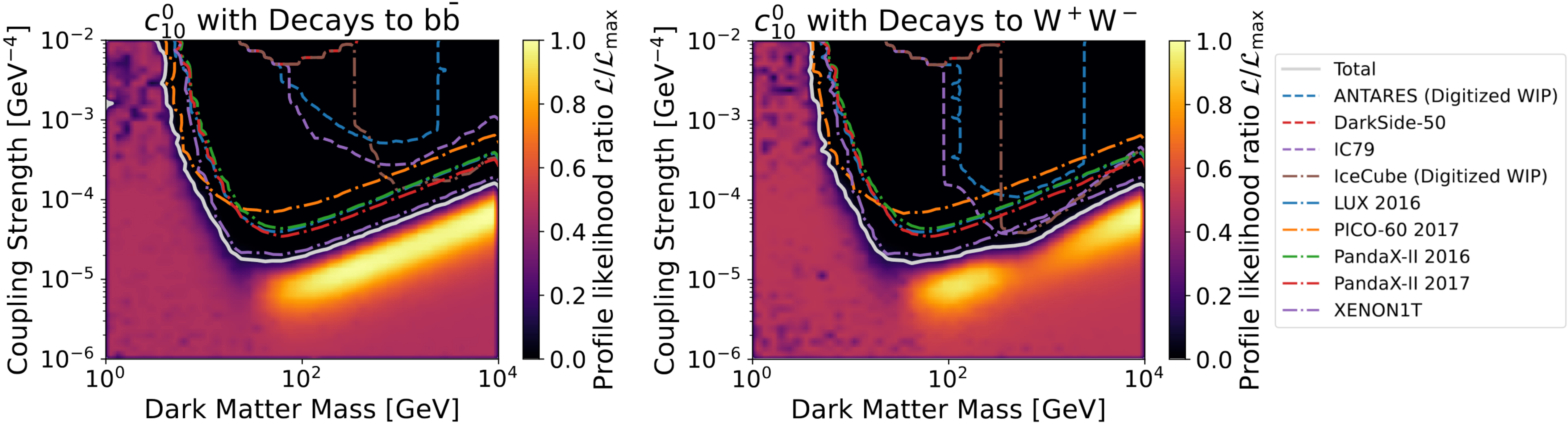

$$\hat{\mathcal{O}}_{10} = i\hat{\mathbf{S}}_N \cdot \frac{\hat{\mathbf{q}}}{m_N}$$

$$\mathcal{L} \supset \lambda_1 \phi\bar{\chi}\chi - ih_2\phi\bar{q}\gamma^5 q \rightarrow \hat{\mathcal{H}} \supset \left(c^0_{10}t^0 + c^1_{10}t^1\right)\hat{\mathcal{O}}_{10}$$

Queen's UNIVERSITY

Conclusions

Conclusions

- Capt'n open to public and has already seen use by GAMBIT community (2106.02056)
- Need accurate modeling of *all isotopes* in the Sun for accurate capture rates!
- This is some of the first set of global constraints on non-relativistic effective operator dark matter from direct detection experiments in addition to solar neutrinos
- IceCube solar neutrinos can assist with spin-dependent direct detection searches
- Whenever new data is added to GAMBIT this work can be re-run with trivial modifications to improve constraints
- This work is currently being modified for use in a Supernova scattering search lead by Christopher Cappiello

Thank You

- [1] M. Schumann, *Direct Detection of WIMP Dark Matter: Concepts and Status, J. Phys. G* **46** (2019) 103003, [arXiv:1903.03026].
- [2] A. L. Fitzpatrick, W. Haxton, E. Katz, N. Lubbers, and Y. Xu, *The Effective Field Theory of Dark Matter Direct Detection, JCAP* **02** (2013) 004, [arXiv:1203.3542].
- [3] J. B. Dent, L. M. Krauss, J. L. Newstead, and S. Sabharwal, *General analysis of direct dark matter detection: From microphysics to observational signatures, Phys. Rev. D* **92** (2015) 063515, [arXiv:1505.03117].
- [4] A. C. Vincent and P. Scott, *Thermal conduction by dark matter with velocity and momentum-dependent cross-sections, JCAP* **04** (2014) 019, [arXiv:1311.2074].
- [5] A. C. Vincent, P. Scott, and A. Serenelli, *Updated constraints on velocity and momentum-dependent asymmetric dark matter, JCAP* **11** (2016) 007, [arXiv:1605.06502].
- [6] J. Lopes and I. Lopes, *Asymmetric Dark Matter Imprint on Low-mass Main-sequence Stars in the Milky Way Nuclear Star Cluster, Astrophys. J.* **879** (2019) 50, [arXiv:1907.05785].
- [7] J. Bramante, *Dark matter ignition of type Ia supernovae, Phys. Rev. Lett.* **115** (2015) 141301, [arXiv:1505.07464].

Queen's UNIVERSITY

Thank You

- [8] J. F. Acevedo, J. Bramante, A. Goodman, J. Kopp, and T. Opferkuch, *Dark Matter, Destroyer of Worlds: Neutrino, Thermal, and Existential Signatures from Black Holes in the Sun and Earth, JCAP* **04** (2021) 026, [arXiv:2012.09176].
- [9] N. F. Bell, G. Busoni, S. Robles, and M. Virgato, *Improved Treatment of Dark Matter Capture in Neutron Stars, JCAP* **09** (2020) 028, [arXiv:2004.14888].
- [10] N. Avis Kozar, A. Caddell, L. Fraser-Leach, P. Scott, and A. C. Vincent, Capt'n General: A generalized stellar dark matter capture and heat transport code, in Tools for High Energy Physics and Cosmology (2021) [arXiv:2105.06810].
- [11] GAMBIT: P. Athron *et. al., GAMBIT: The Global and Modular Beyond-the-Standard-Model Inference Tool, Eur. Phys. J. C* **77** (2017) 784, [arXiv:1705.07908]. [Addendum: Eur.Phys.J.C 78, 98 (2018)].
- [12] IceCube: P. Scott *et. al., Use of event-level neutrino telescope data in global fits for theories of new physics, JCAP* **11** (2012) 057, [arXiv:1207.0810].
- [13] IceCube: R. Abbasi *et. al., The Design and Performance of IceCube DeepCore, Astropart. Phys.* **35** (2012) 615–624, [arXiv:1109.6096].
- [14] IceCube: M. G. Aartsen *et. al., Search for Neutrinos from Dark Matter Self-Annihilations in the center of the Milky Way with 3 years of IceCube/DeepCore, Eur. Phys. J. C* 77 (2017) 627, [arXiv:1705.08103].
- [15] LUX: D. S. Akerib *et. al., Results from a search for dark matter in the complete LUX exposure, Phys. Rev. Lett.* **118** (2017) 021303, [arXiv:1608.07648].

Thank You

- [16] XENON: E. Aprile *et. al., Dark Matter Search Results from a One Ton-Year Exposure of XENON1T, Phys. Rev. Lett.* **121** (2018) 111302, [arXiv:1805.12562].
- [17] PandaX-II: A. Tan *et. al., Dark Matter Results from First 98.7 Days of Data from the PandaX-II Experiment, Phys. Rev. Lett.* **117** (2016) 121303, [arXiv:1607.07400].
- [18] PandaX-II: X. Cui *et. al., Dark Matter Results From 54-Ton-Day Exposure of PandaX-II Experiment, Phys. Rev. Lett.* **119** (2017) 181302, [arXiv:1708.06917].
- [19] PICO: C. Amole *et. al., Dark Matter Search Results from the PICO-60 C3F8 Bubble Chamber, Phys. Rev. Lett.* **118** (2017) 251301, [arXiv:1702.07666].
- [20] CRESST: G. Angloher *et. al., Results on light dark matter particles with a low-threshold CRESST-II detector, Eur. Phys. J. C* 76 (2016) 25, [arXiv:1509.01515].
- [21] SuperCDMS: R. Agnese *et. al., New Results from the Search for Low-Mass Weakly Interacting Massive Particles with the CDMS Low Ionization Threshold Experiment, Phys. Rev. Lett.* **116** (2016) 071301, [arXiv:1509.02448].
- [22] DarkSide: P. Agnes *et. al., DarkSide-50 532-day Dark Matter Search with Low-Radioactivity Argon, Phys. Rev. D* **98** (2018) 102006, [arXiv:1802.07198].

Queen's UNIVERSITY

Thank You

- [23] ANTARES: C. Poirè, *Limits for Dark Matter annihilation in the Sun with ANTARES neutrino telescope, Dark Ghosts* 2022, [PDF]
- [24] IceCube: S. Meighen-Berger, *Dark Matter Searches with IceCube, Dark Ghosts* 2022, [PDF]
- [25] GAMBIT: G. D. Martinez, J. McKay, *et. al.*, *Comparison of statistical sampling methods with ScannerBit, the GAMBIT scanning module*, *Eur. Phys. J.* C 77 (2017) 761, [arXiv:1705.07959].
- [26] *R. Catena and B. Schwabe, Form factors for dark matter capture by the Sun in effective theories, JCAP* **04** (2015) 042, [arXiv:1501.03729].

Queen's UNIVERSITY

Queen's UNIVERSITY

Backup Slides

Capt’n Comparisons c_1

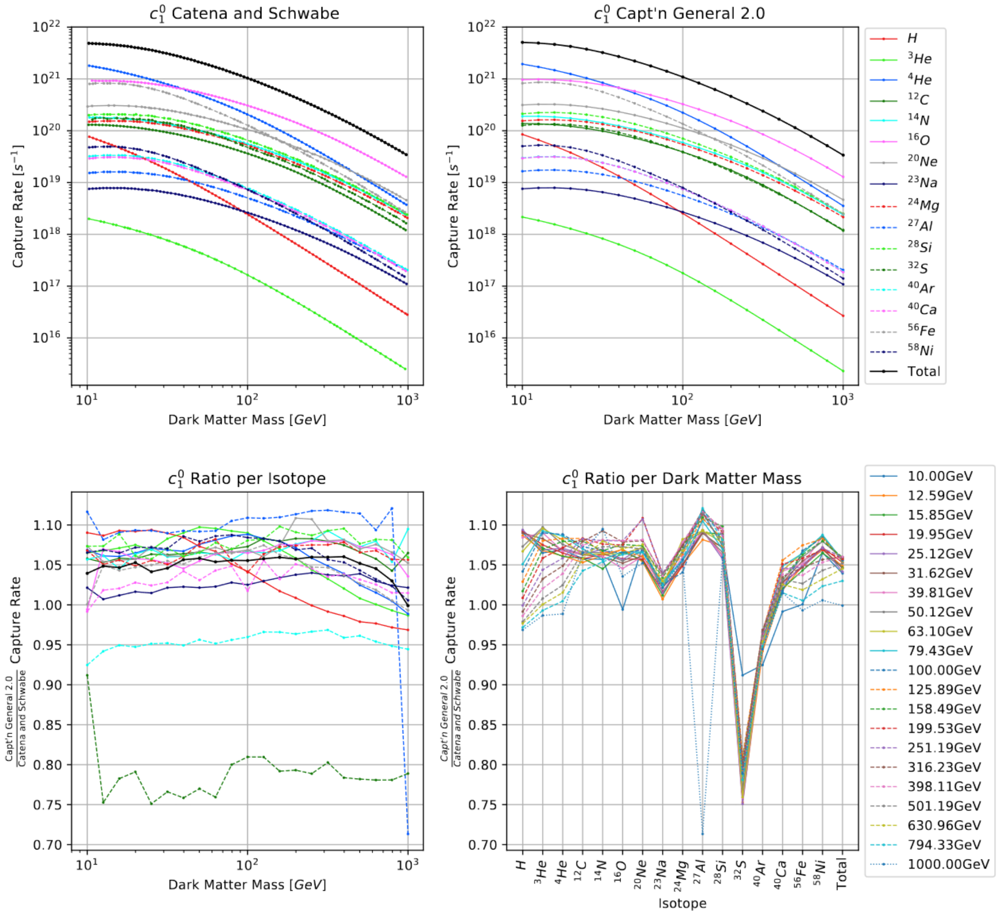

Capt’n Comparisons c_3

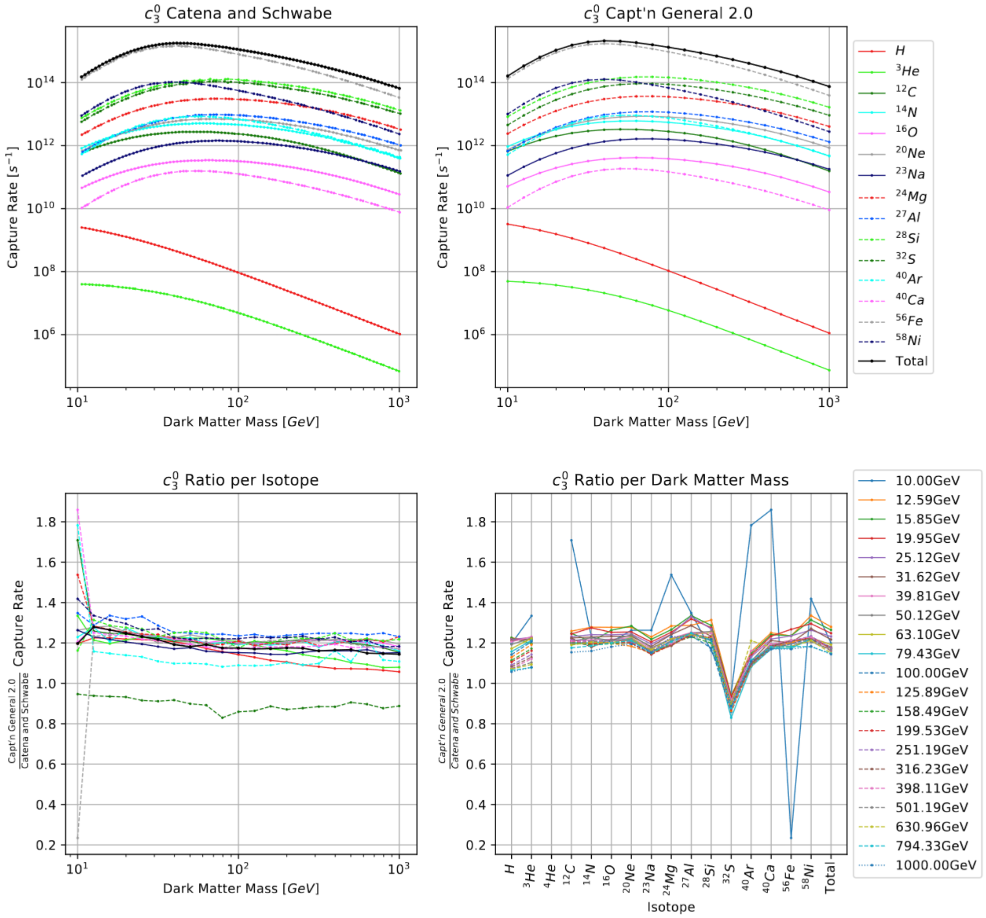

Capt’n Comparisons c_4

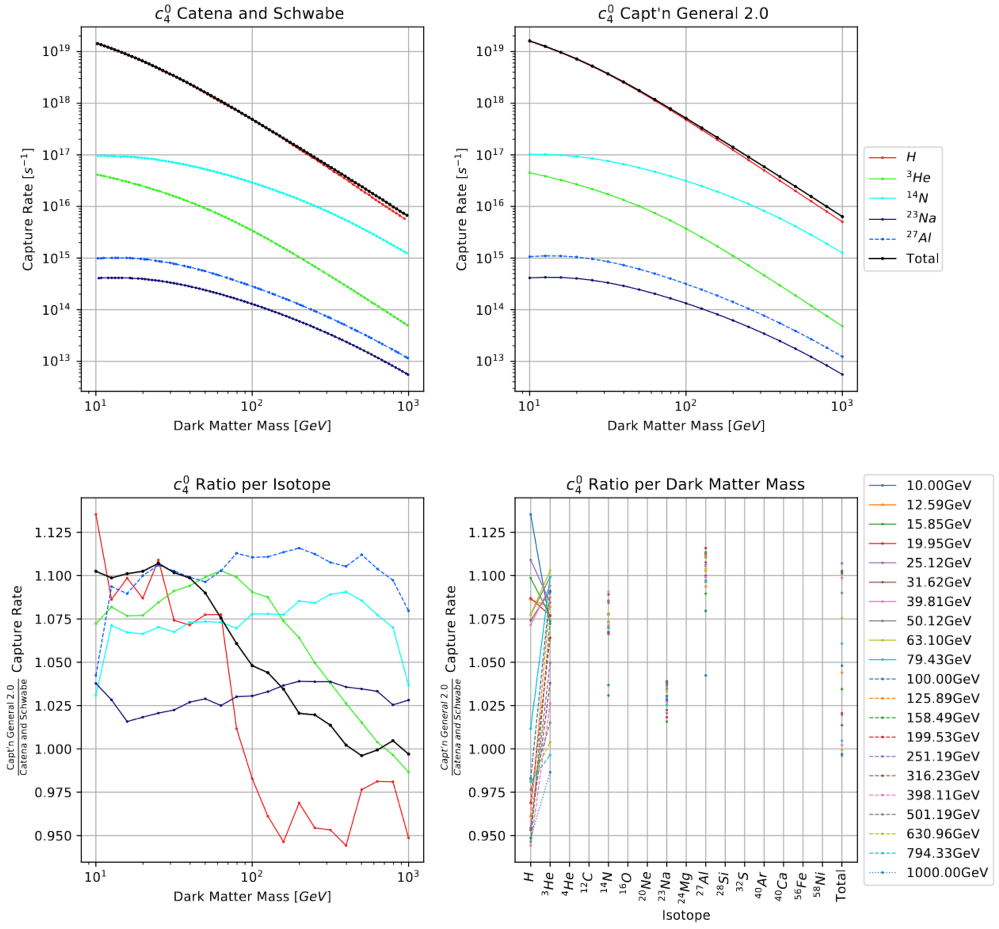

Capt’n Comparisons c_5

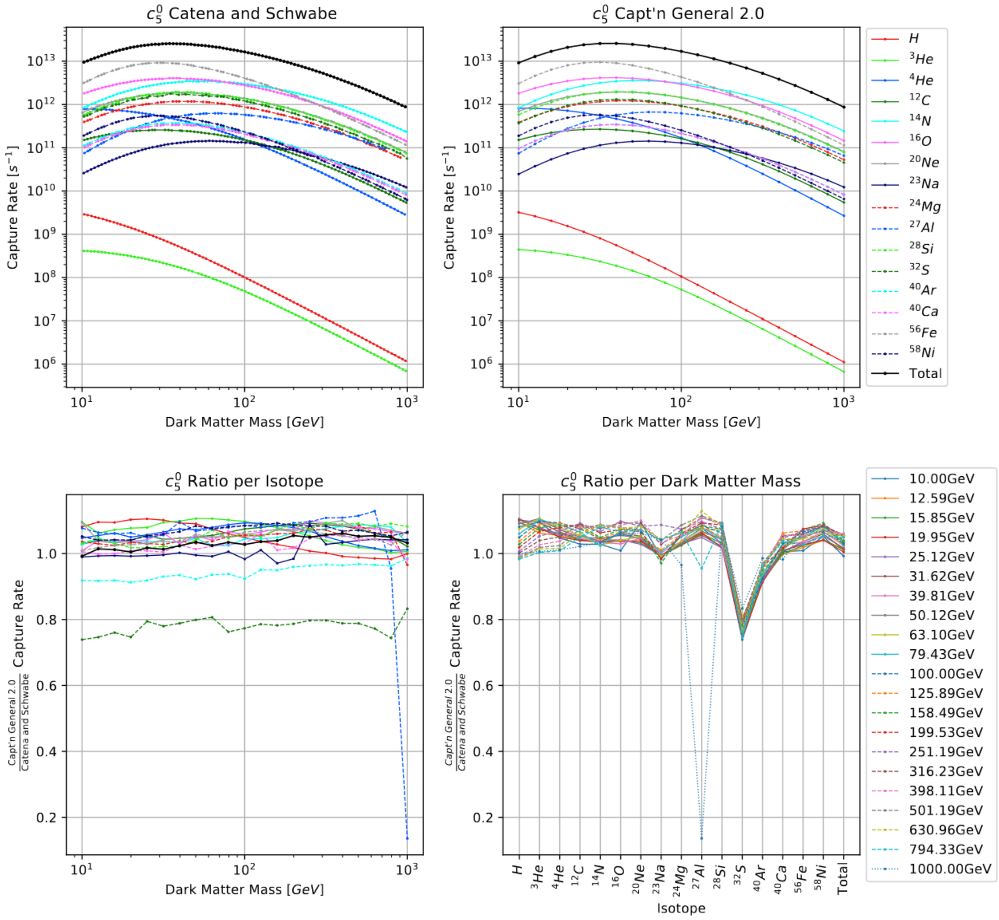

Capt'n Comparisons c_6

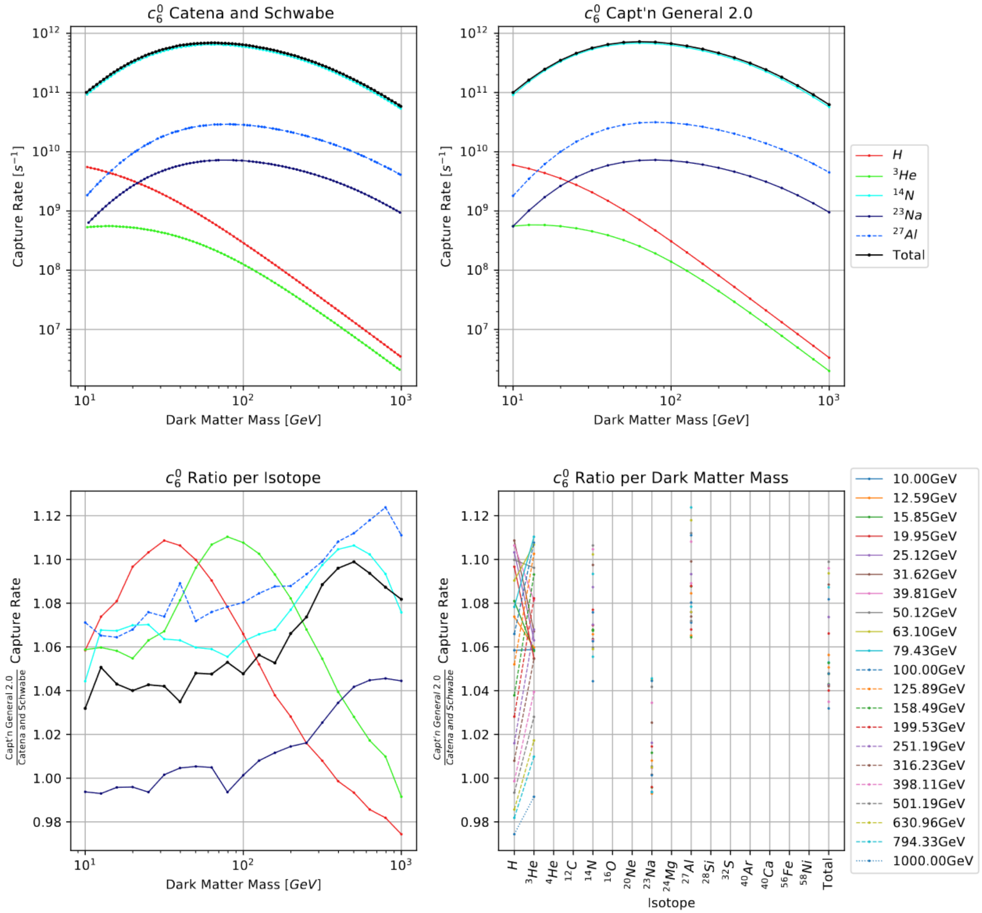

Capt'n Comparisons c_7

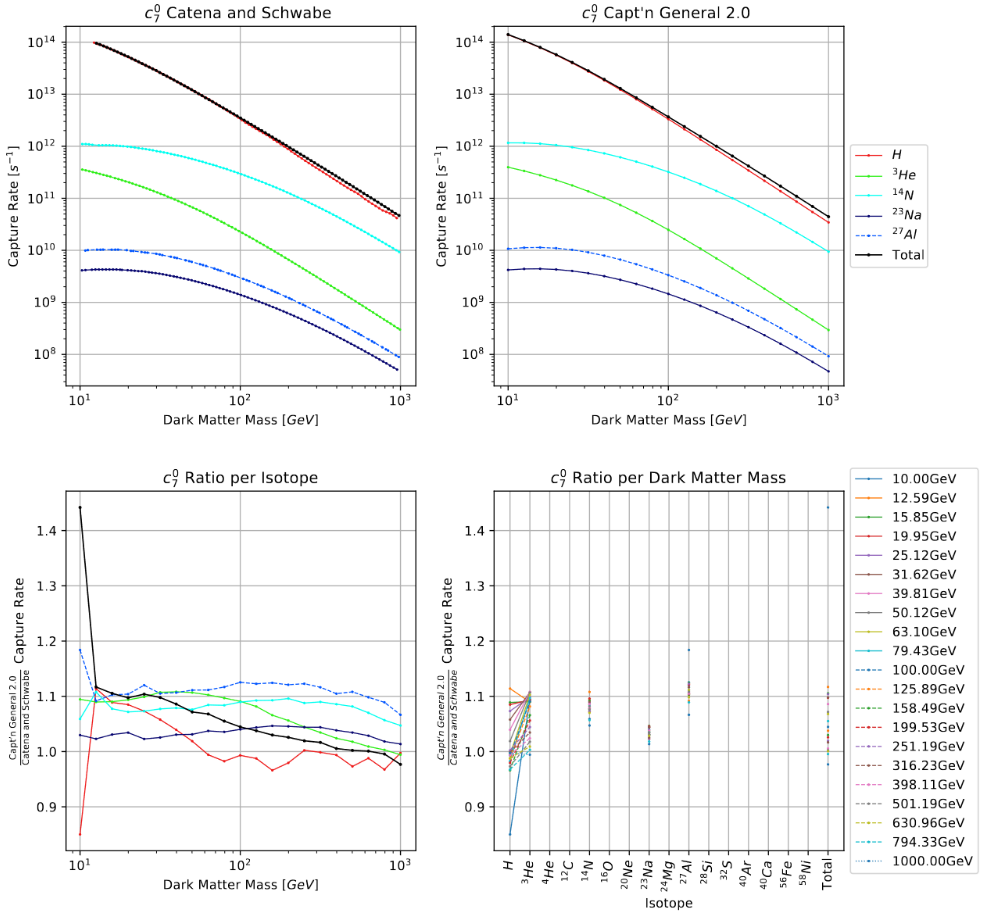

Capt’n Comparisons c_8

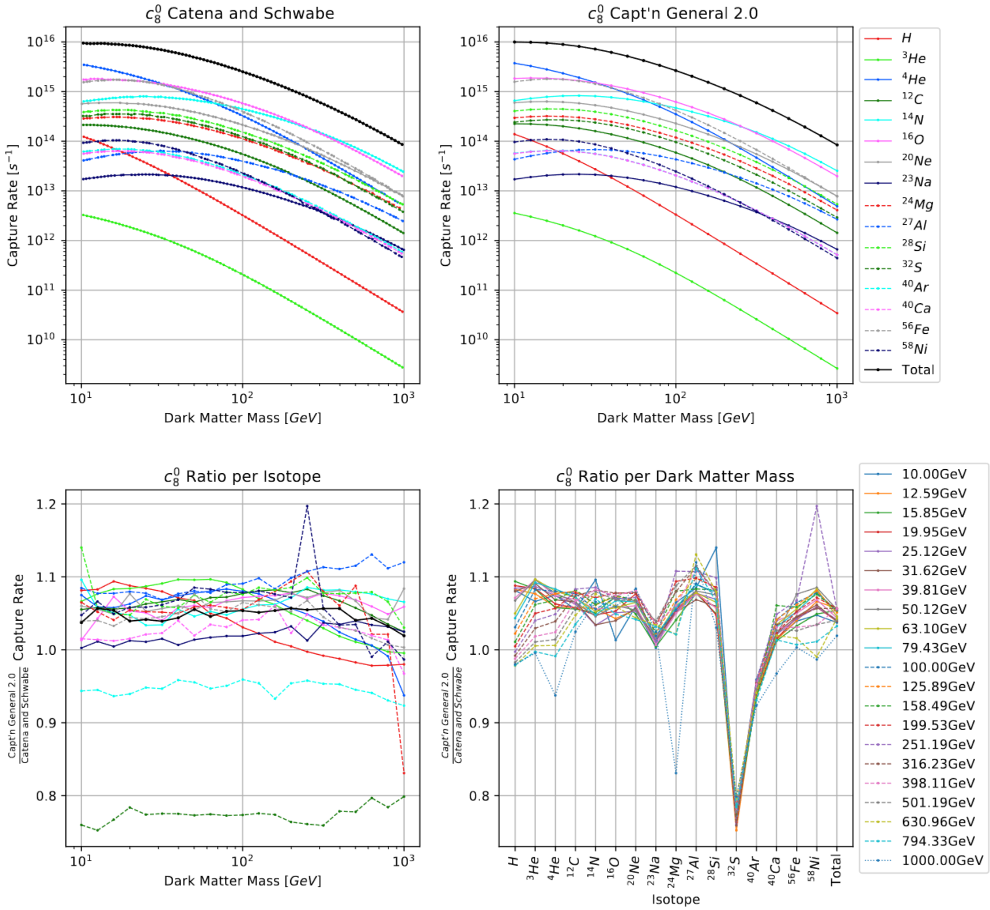

Capt'n Comparisons c_9

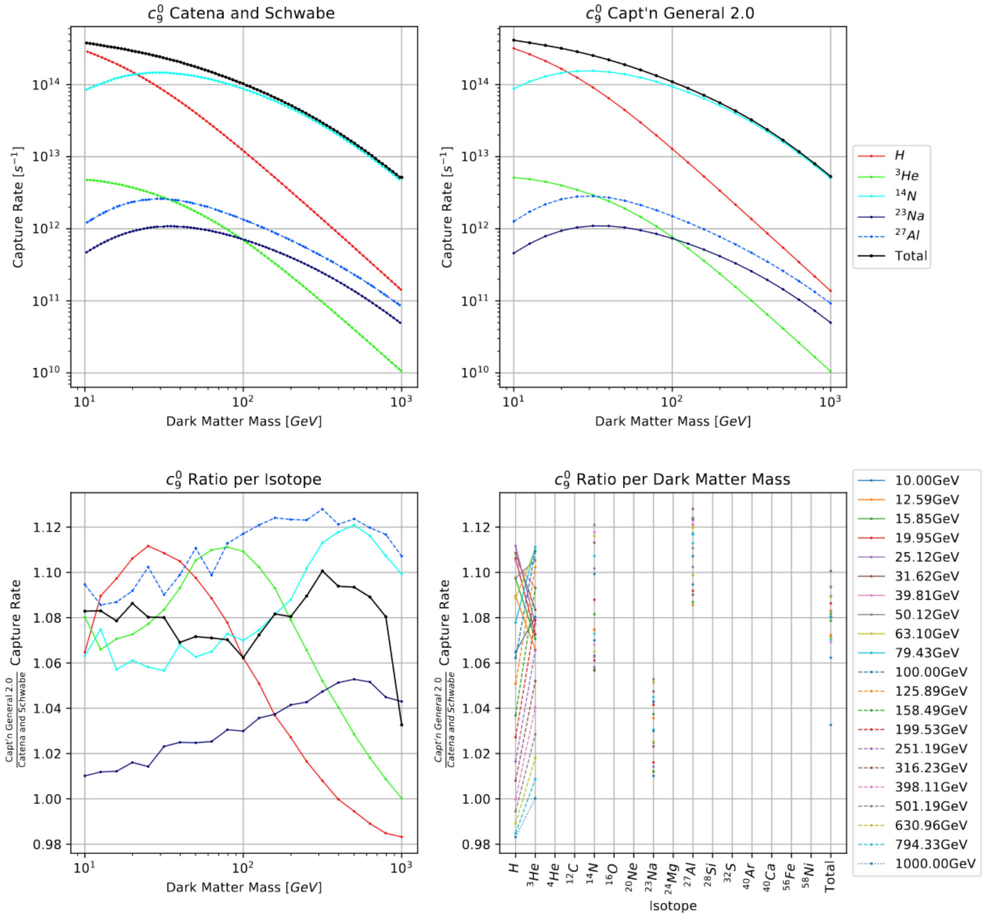

Capt'n Comparisons c_{10}

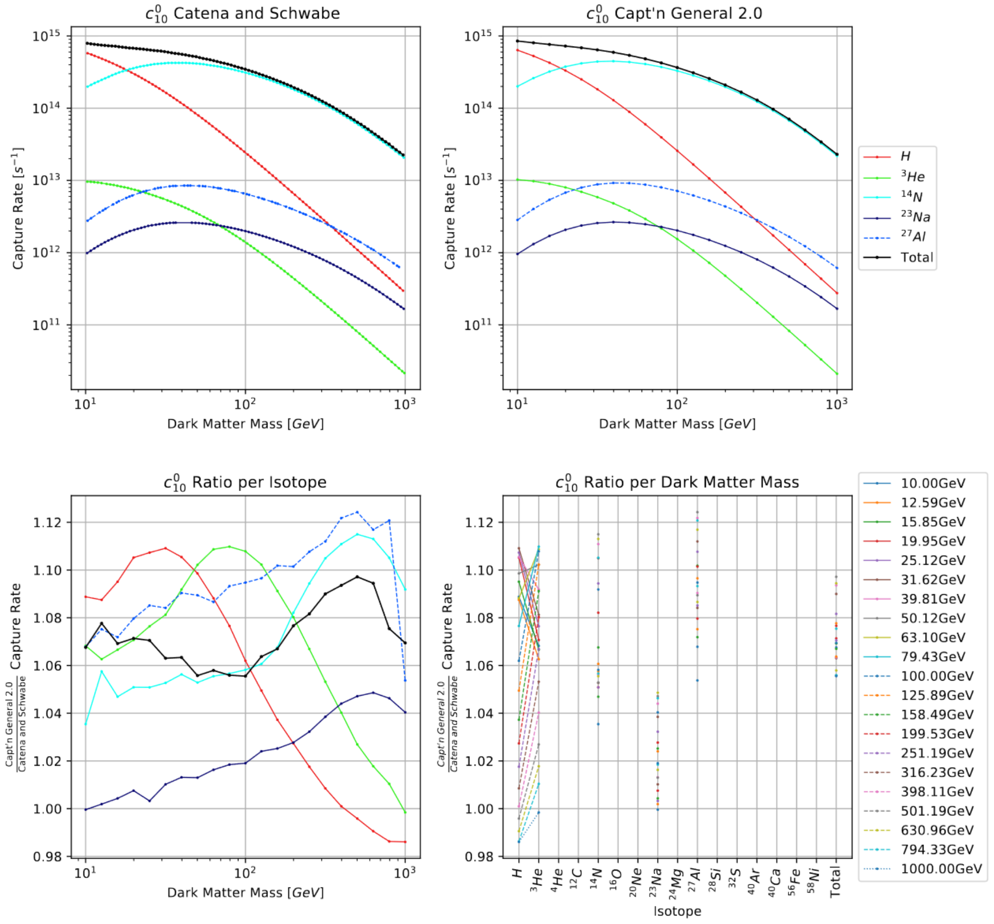

Capt’n Comparisons c_{11}

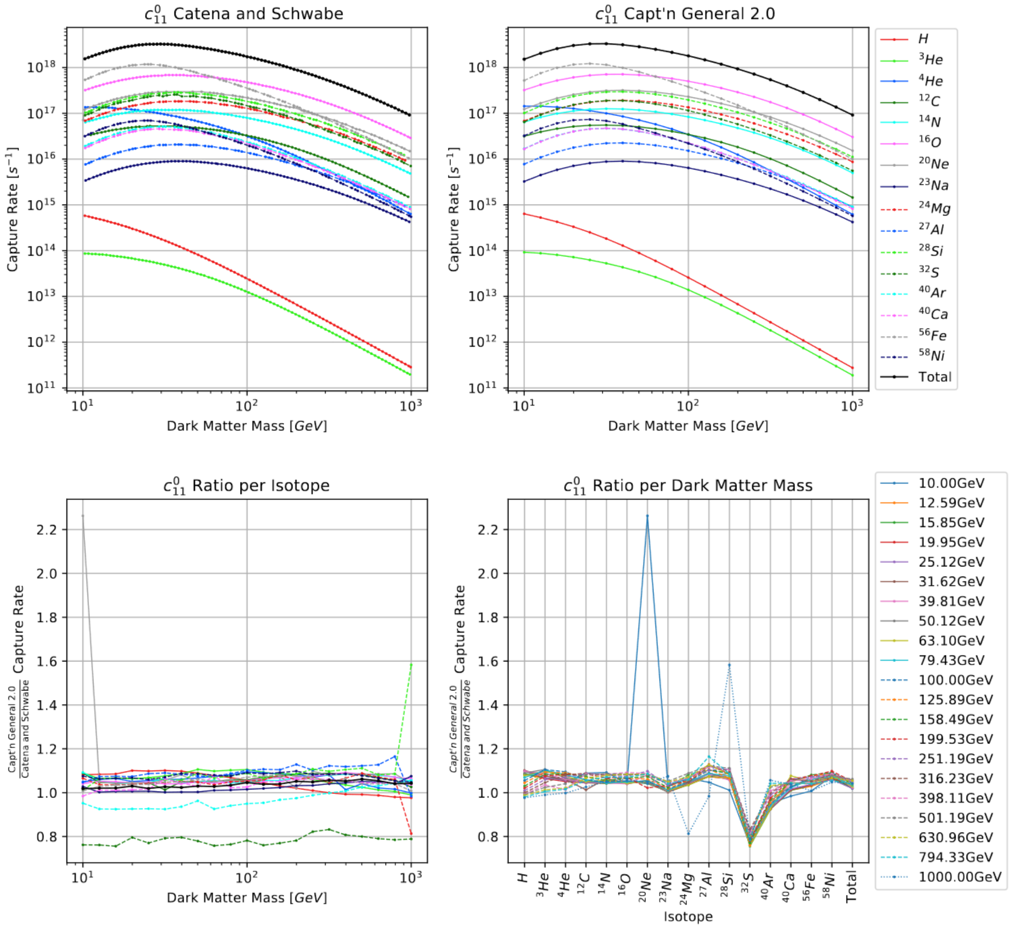

Capt’n Comparisons c_{12}

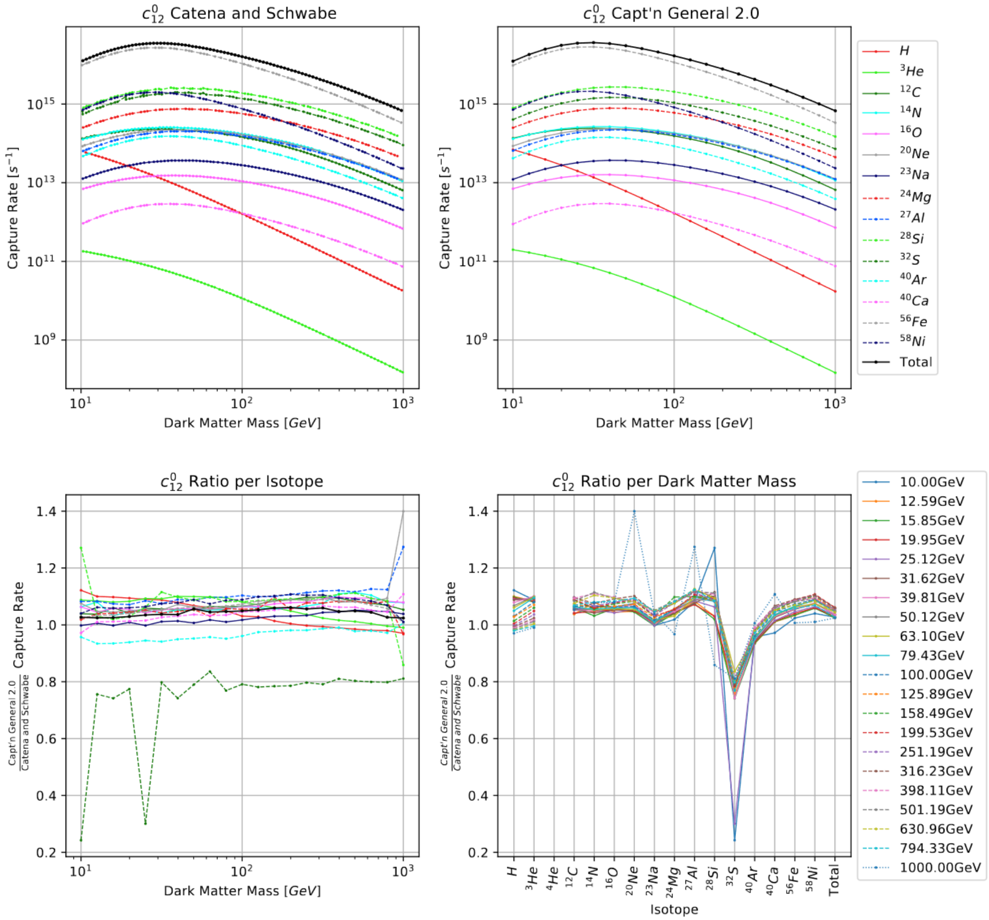

Capt’n Comparisons c_{13}

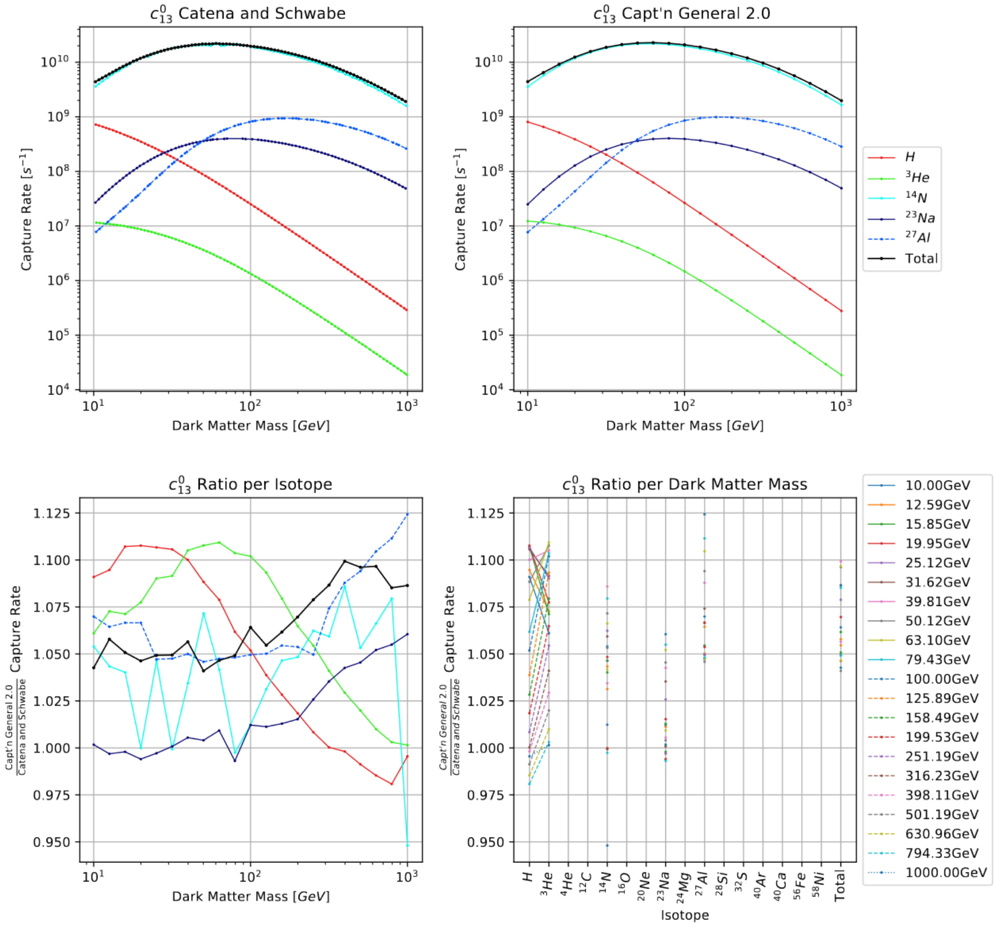

Capt’n Comparisons c_{14}

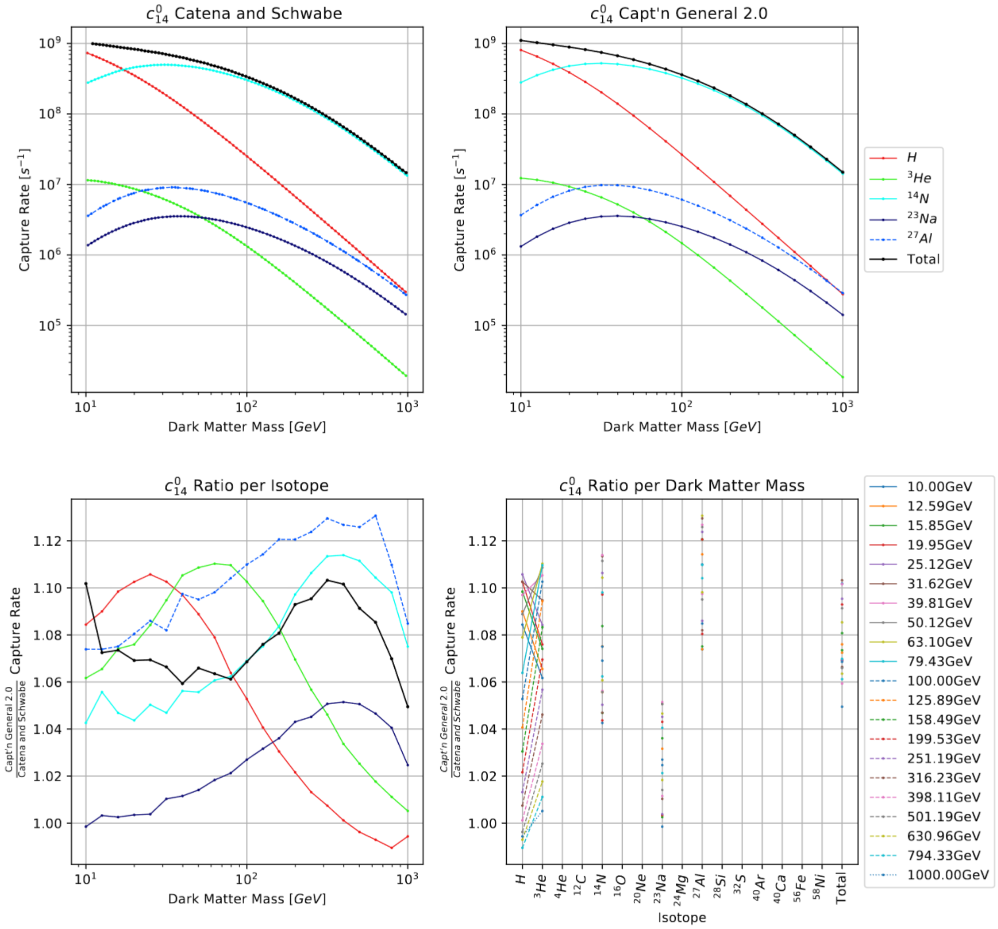

Capt’n Comparisons c_{15}

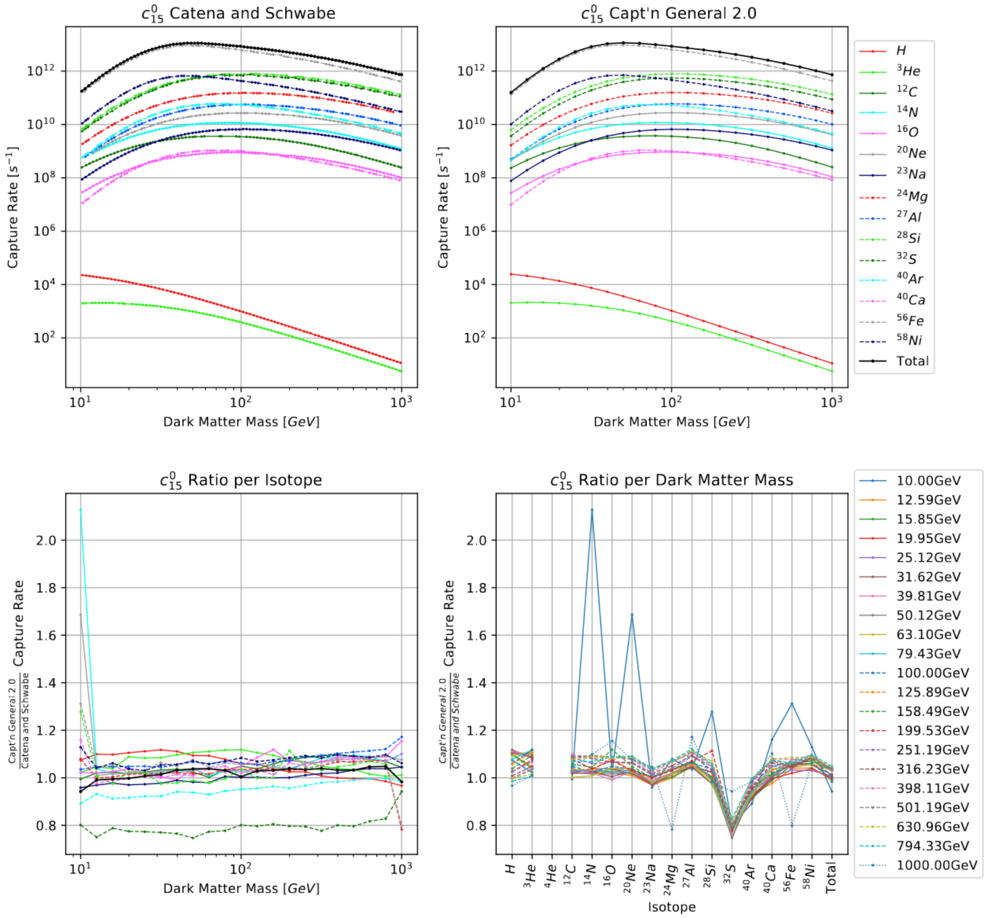

GAMBIT-Capt’n Dependency

- Capt’n acts as a backend of DarkBit
- It is used to calculate the capture rate for GAMBIT

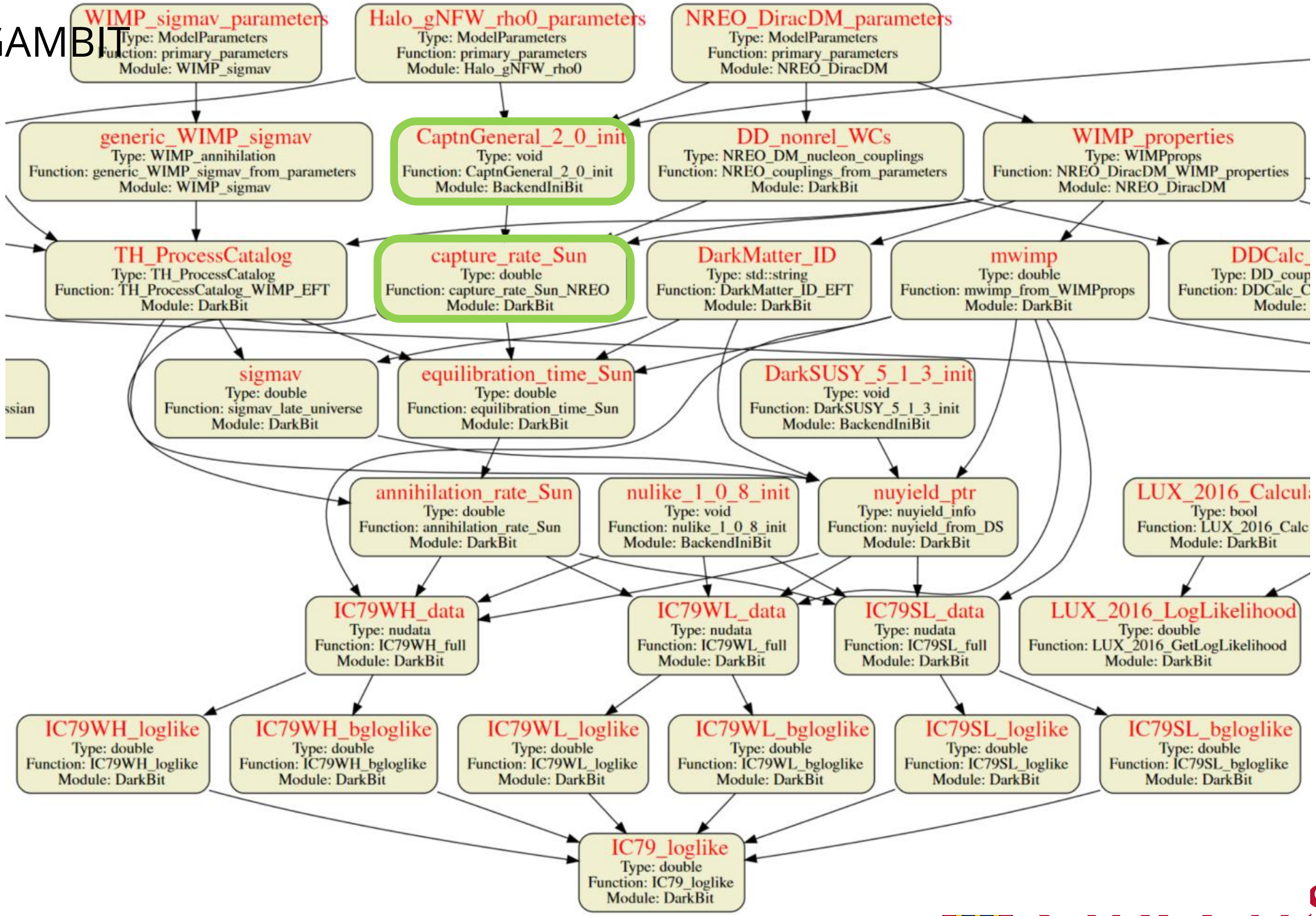

GAMBIT Direct Detection

- DDCalc acts to translate the couplings to cross sections for the DD experiments

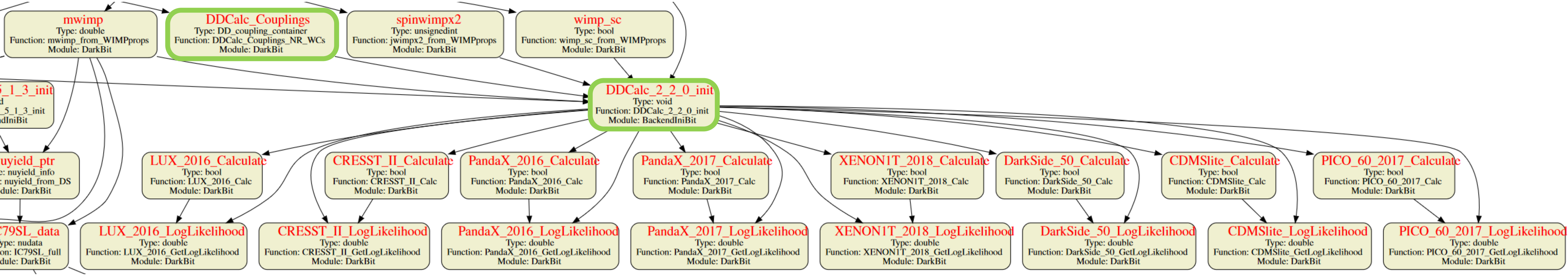

All Coupling Parameters

Dark Matter Parameters			
m_{dm}	1 - 10^4 GeV		
c_1^0	10^{-10} - 10^{-6} GeV^{-2}	c_9^0	10^{-6} - 10^{-2} GeV^{-2}
c_3^0	10^{-7} - 10^{-3} GeV^{-2}	c_{10}^0	10^{-6} - 10^{-2} GeV^{-2}
c_4^0	10^{-8} - 10^{-4} GeV^{-2}	c_{11}^0	10^{-9} - 10^{-5} GeV^{-2}
c_5^0	10^{-6} - 10^{-2} GeV^{-2}	c_{12}^0	10^{-8} - 10^{-4} GeV^{-2}
c_6^0	10^{-5} - 10^{-1} GeV^{-2}	c_{13}^0	10^{-6} - 10^{-2} GeV^{-2}
c_7^0	10^{-5} - 10^{-1} GeV^{-2}	c_{14}^0	10^{-5} - 10^{-1} GeV^{-2}
c_8^0	10^{-7} - 10^{-3} GeV^{-2}	c_{15}^0	10^{-5} - 10^{-1} GeV^{-2}

c_3 $b\bar{b}$ and W^+W^- Channels

- c_3 $b\bar{b}$ left and W^+W^- right

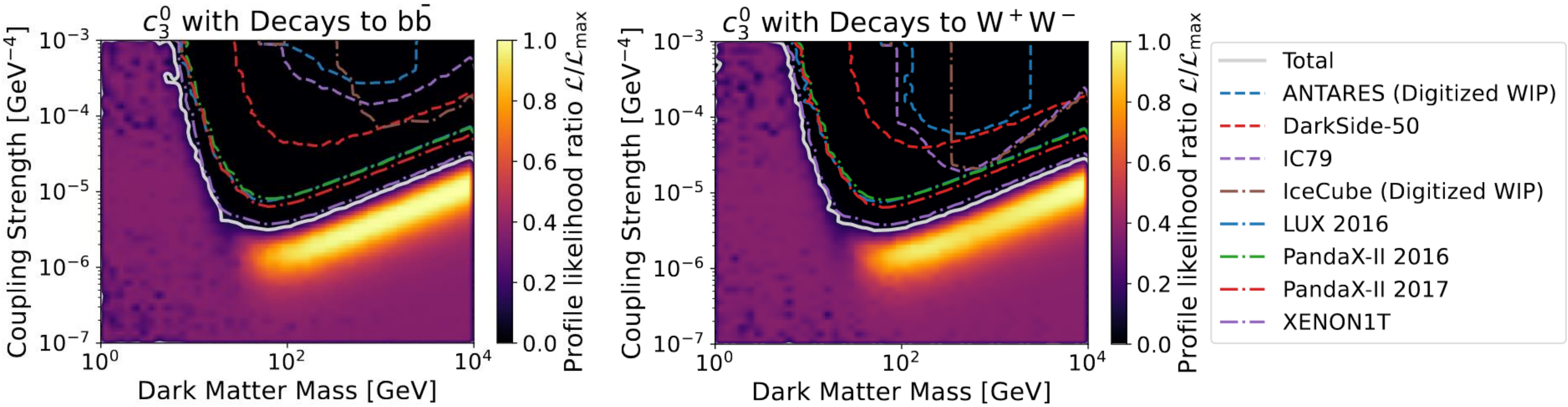

c_5 $b\bar{b}$ and W^+W^- Channels

- c_5 $b\bar{b}$ left and W^+W^- right

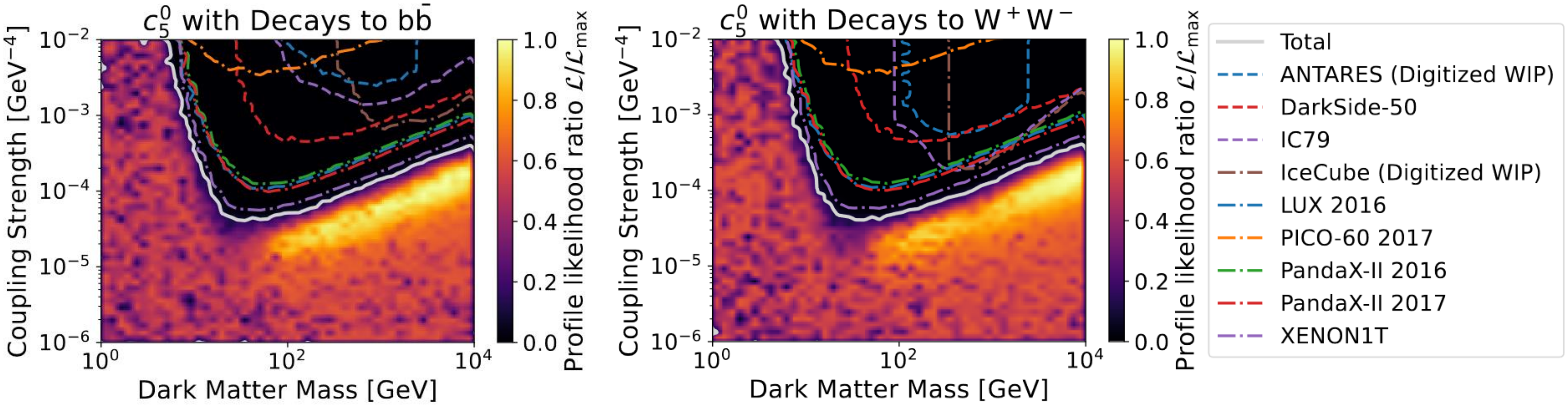

c_6 $b\bar{b}$ and W^+W^- Channels

- c_6 $b\bar{b}$ left and W^+W^- right

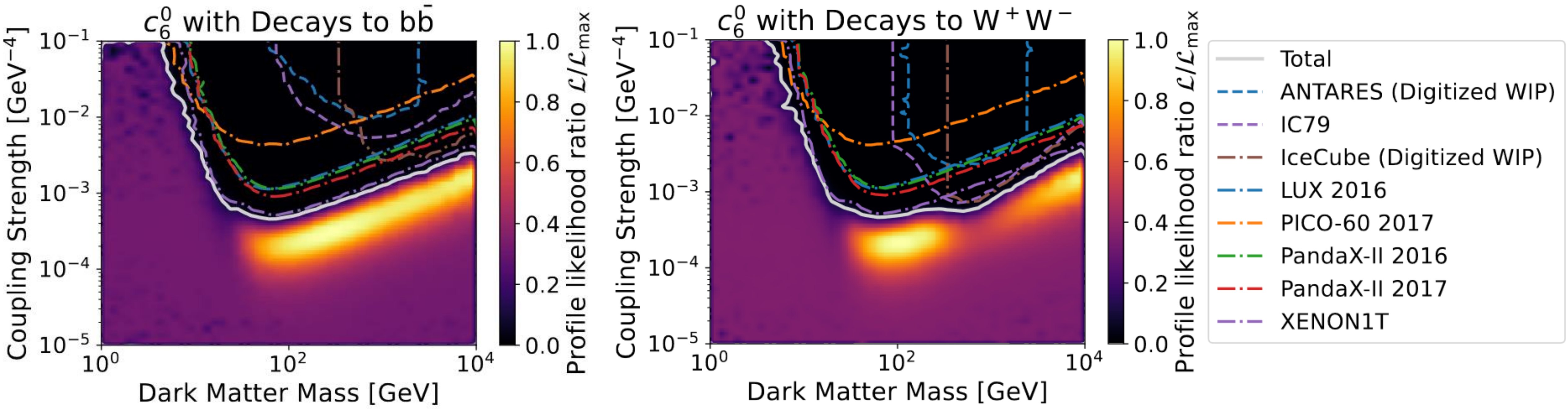

c_7 $b\bar{b}$ and W^+W^- Channels

- c_7 $b\bar{b}$ left and W^+W^- right

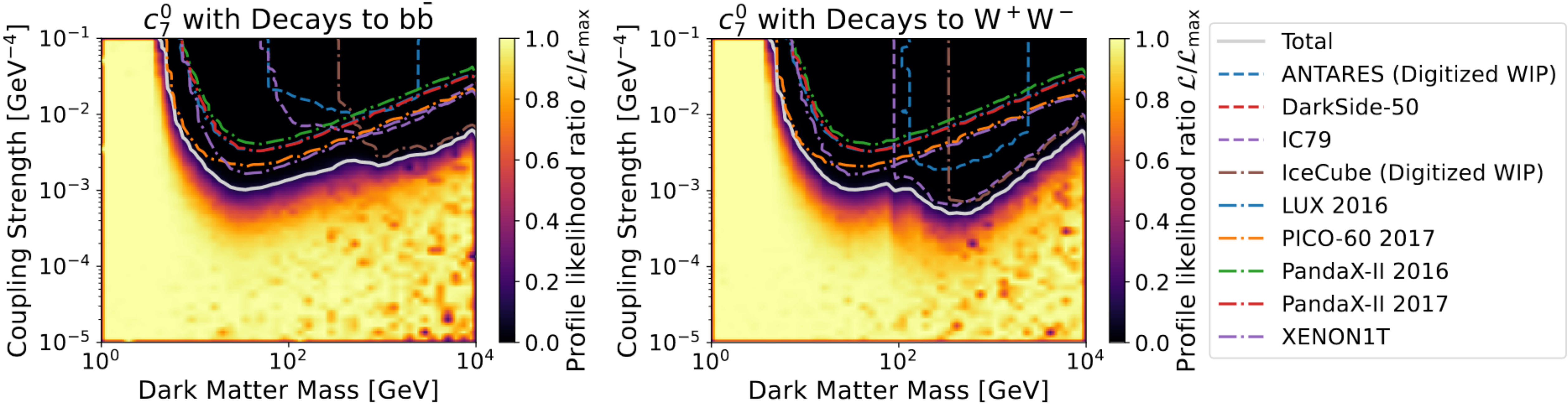

c_8 $b\bar{b}$ and W^+W^- Channels

- c_8 $b\bar{b}$ left and W^+W^- right

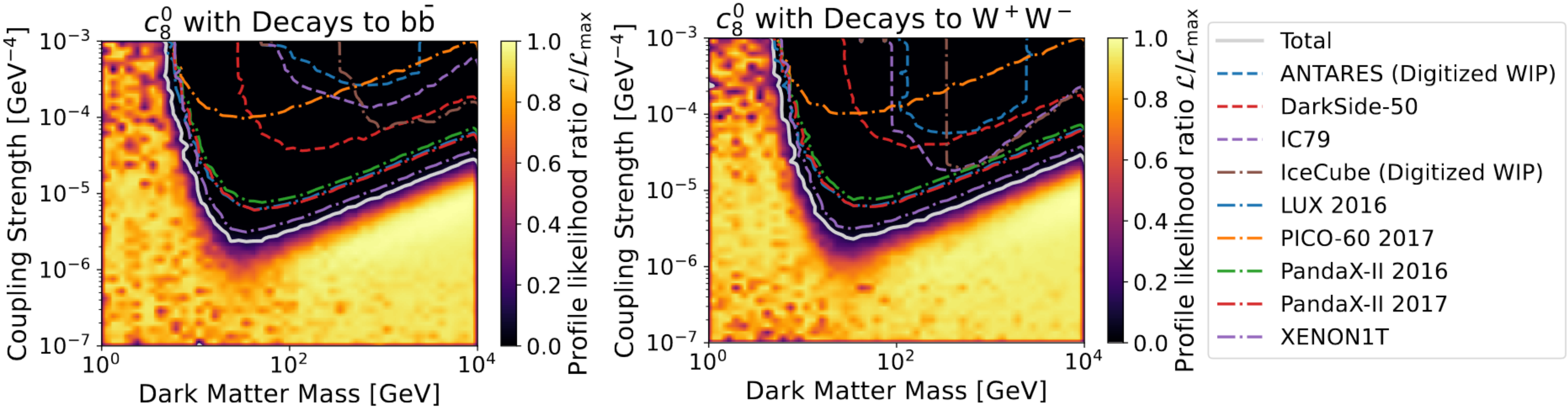

c_9 $b\bar{b}$ and W^+W^- Channels

- c_9 $b\bar{b}$ left and W^+W^- right

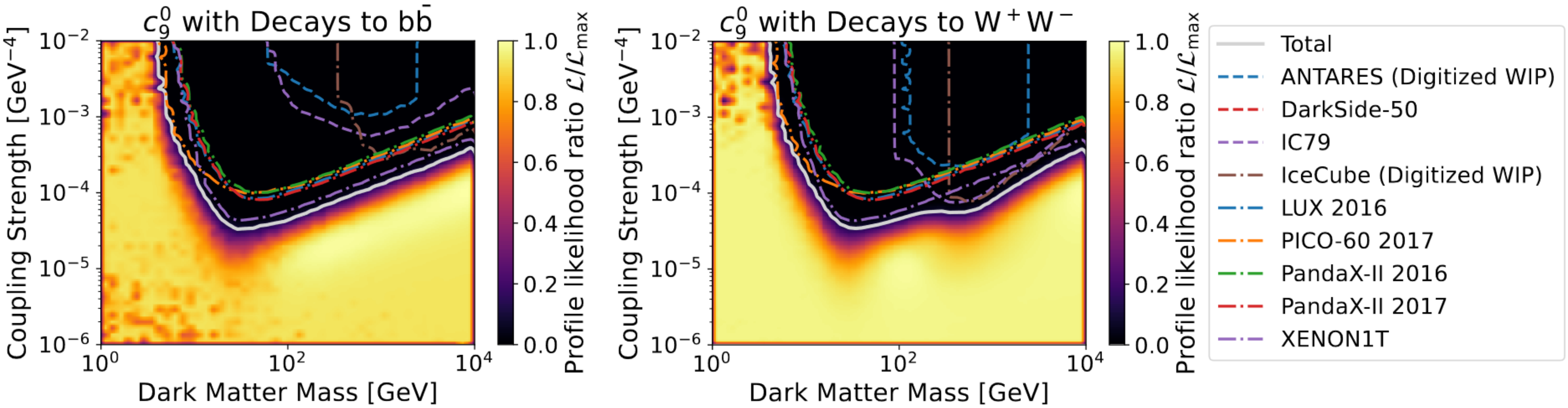

c_{10} $b\bar{b}$ and W^+W^- Channels

- c_{10} $b\bar{b}$ left and W^+W^- right

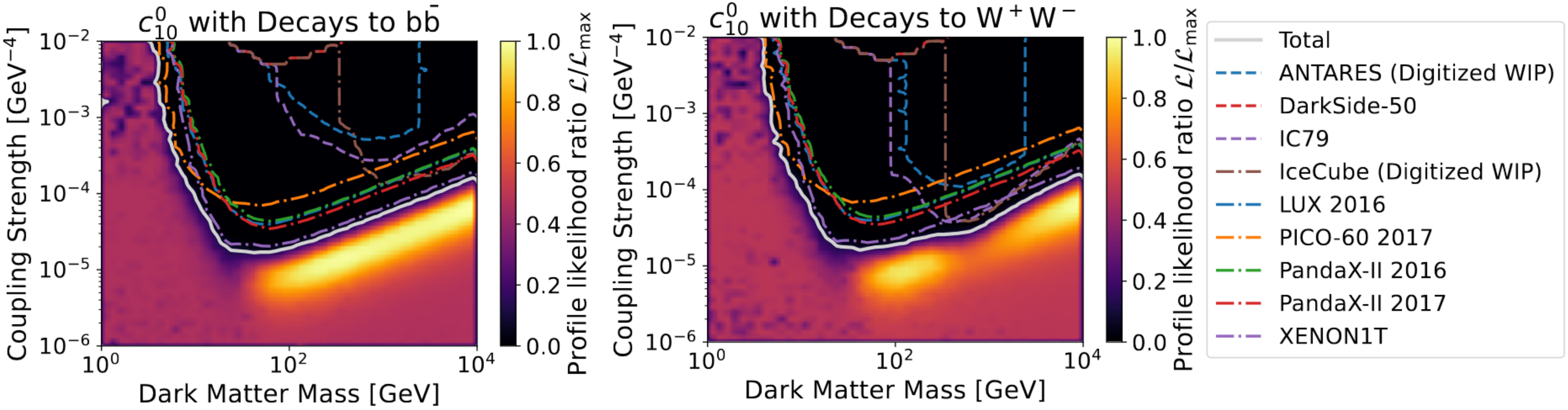

c_{11} $b\bar{b}$ and W^+W^- Channels

- c_{11} $b\bar{b}$ left and W^+W^- right

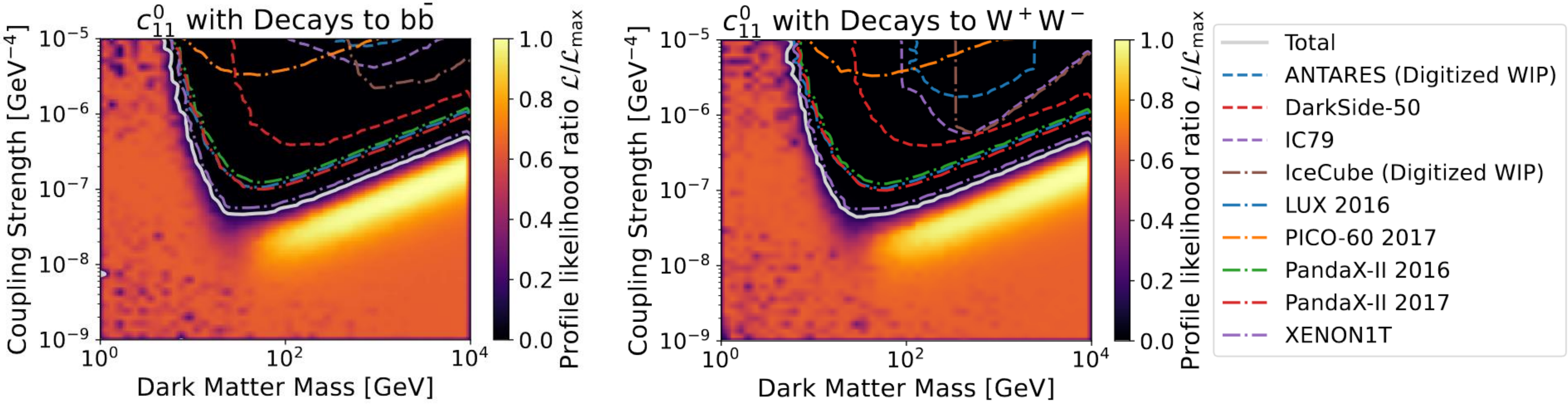

c_{12} $b\bar{b}$ and W^+W^- Channels

- c_{12} $b\bar{b}$ left and W^+W^- right

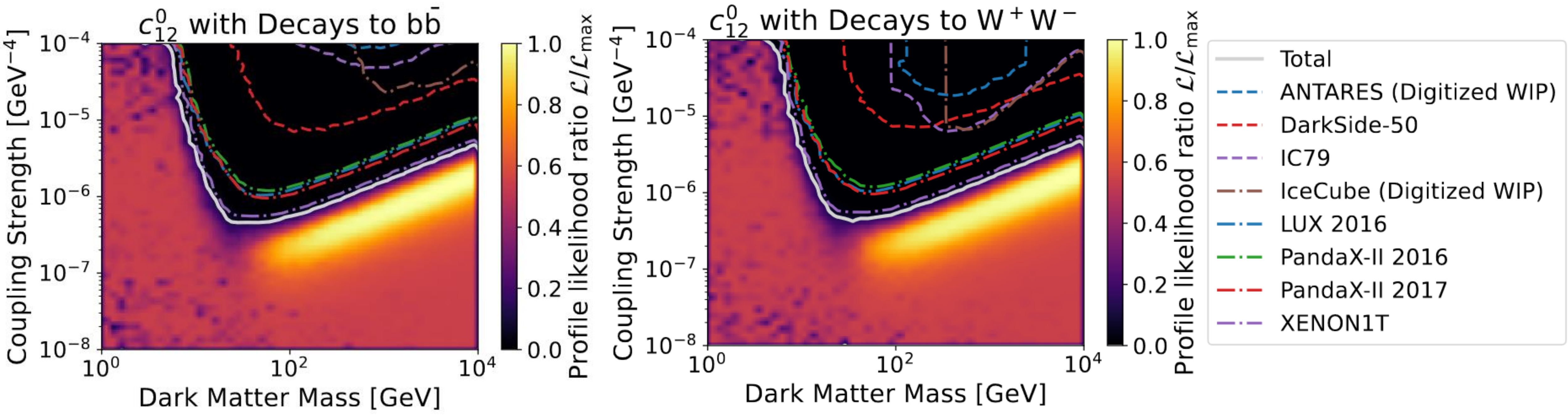

c_{13} $b\bar{b}$ and W^+W^- Channels

- c_{13} $b\bar{b}$ left and W^+W^- right

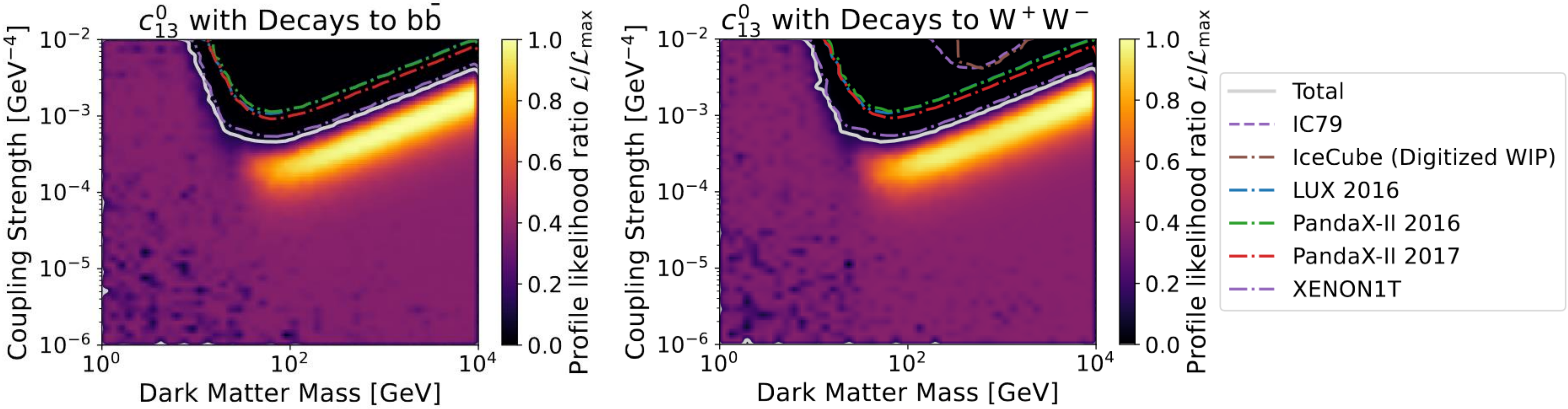

c_{14} $b\bar{b}$ and W^+W^- Channels

- c_{14} $b\bar{b}$ left and W^+W^- right

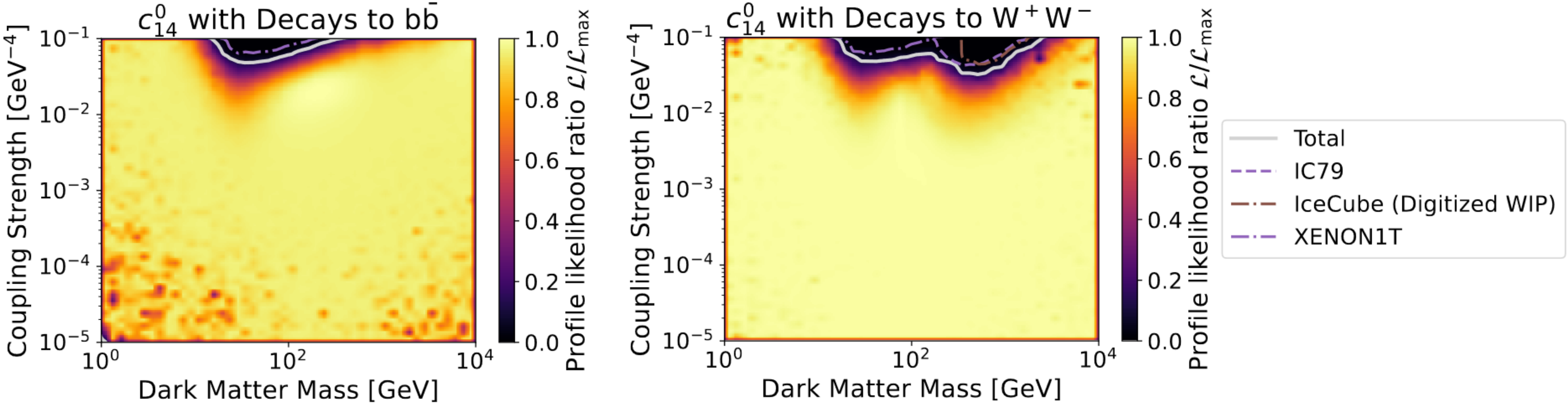

c_{15} $b\bar{b}$ and W^+W^- Channels

- c_{15} $b\bar{b}$ left and W^+W^- right

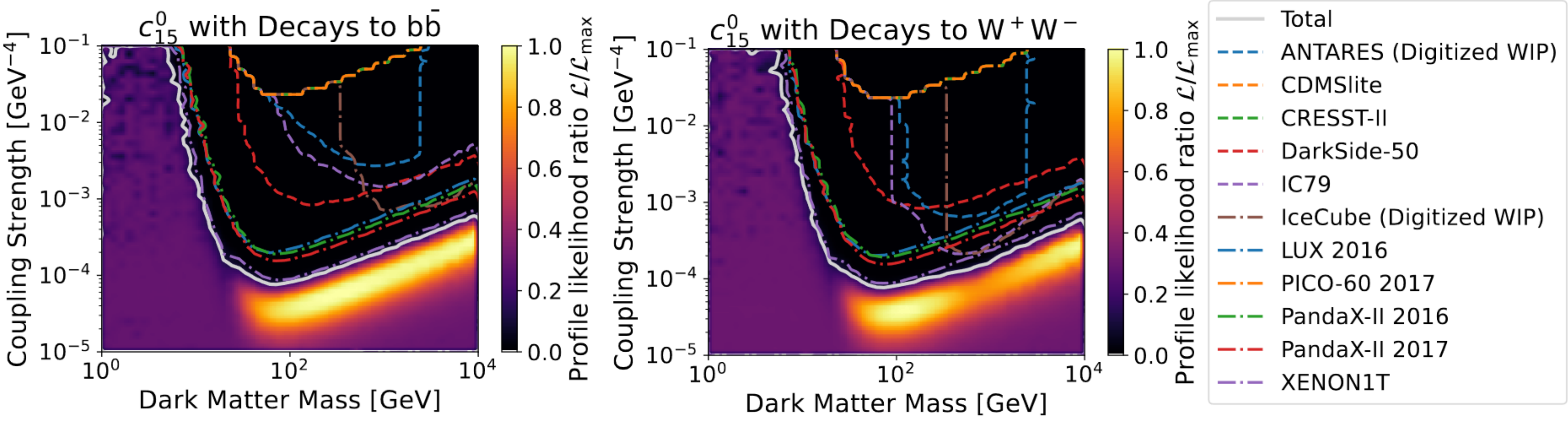

Nuisance Parameters

- The nuisance parameters showed no preference

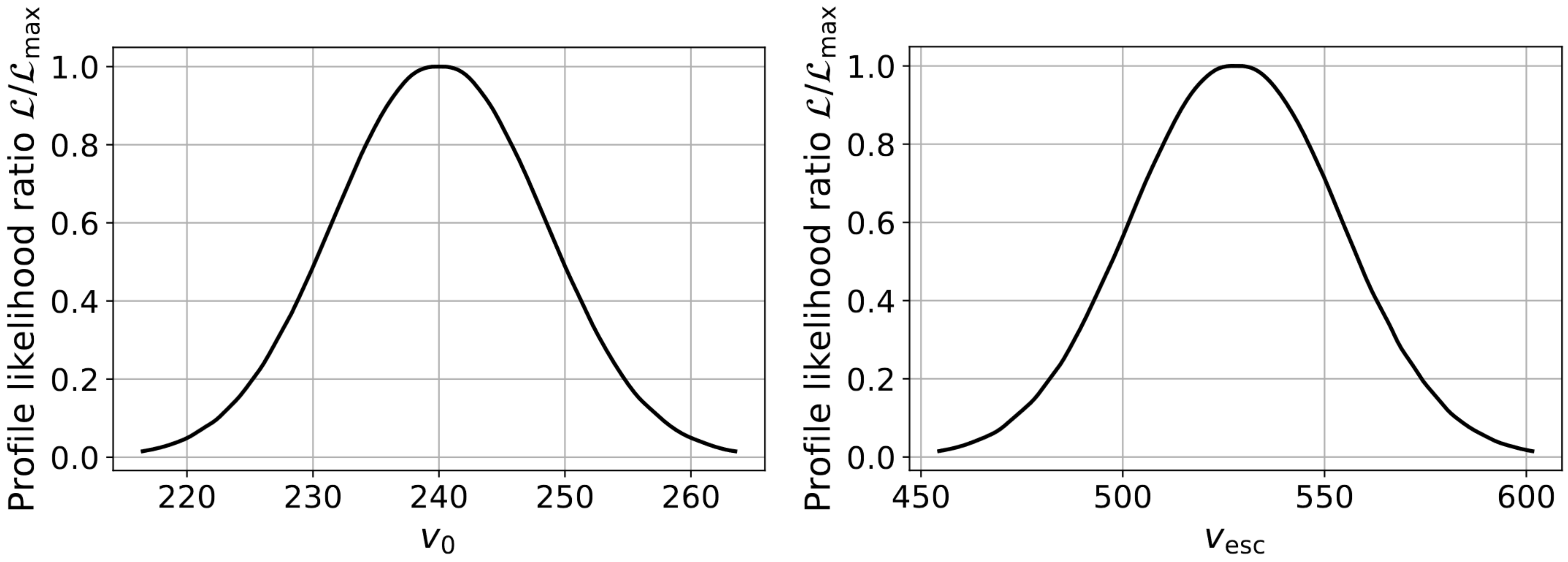

Queen's
UNIVERSITY